FOURTH
QUARTERLY REPORT

EVALUATION AND DEMONSTRATION OF THE USE
OF CRYOGENIC PRPOPELLANTS(O_2-H_2) FOR
REACTION CONTROL SYSTEMS

Prepared for

NATIONAL AERONAUTICS AND SPACE ADMINISTRATION

13 July 1966

CONTRACT NAS3-7941

Technical Management
NASA Lewis Research Center
Cleveland, Ohio

ROCKETDYNE
A Division of North American Aviation, Inc.
6633 Canoga Avenue, Canoga Park, California

EVALUATION AND DEMONSTRATION OF THE USE
OF CRYOGENIC PROPELLANTS (O_2-H_2) FOR
REACTION CONTROL SYSTEMS

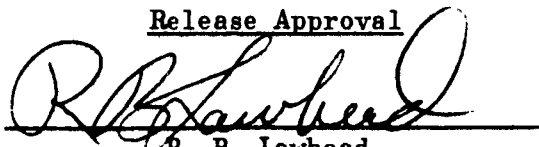Technically Reviewed and Approved by:

G. L. Falkenstein
Principal Scientist
Small Thrustor Systems and Controls

E. V. Zettle
Group Scientist
Propulsion Applications

Release Approval

R. B. Lawhead
Section Chief
Propulsion Processes and Applications

FOREWORD

This quarterly progress report was prepared for the NASA
Lewis Research Center, Cleveland, Ohio, by Rocketdyne,
a Division of North American Aviation, Inc., Canoga Park,
California. The effort was conducted under Contract
NAS3-7941 and G.O. 8734. This report covers the
period 1 April 1966 through 1 July 1966.

ACKNOWLEDGMENT

The following engineering personnel participated in the
technical effort and report preparation for the fourth
quarter contract effort:

N. Weber	Thrustor
N. Rodewald	Conditioner and Thrustor Analysis
E. Prono	Conditioner Analysis and Design
G. Haroldsen	Conditioner Analysis
F. Hunter	Thrustor Design
A. Liebman	Thrustor and Conditioner Analysis
C. Falkenstein	Thrustor Conditioner

PRECEDING PAGES BLANK-NOT FILMED

CONTENTS

TABLES

ILLUSTRATIONS

INTRODUCTION AND SUMMARY

A 16-month applied research program is being conducted with the overall objectives of evaluating and demonstrating the feasibility of a cryogenic reaction control system (RCS) and exploring possible problem areas of such a system. This is to be accomplished by means of detailed analyses and design evaluations for new component and system concepts, along with a supporting experimental program. The possible ultimate use of the system for manned spacecraft as well as unmanned upperstage applications is to be considered as a basis for the preliminary design portion of the program.

The RCS is divided into two subsystems. One subsystem is to condition the propellants to a given thermodynamic state regardless of the inlet state; the other subsystem consists of the thrustors. The program consists of six integrated tasks (an initial concept design-analytical effort; a design, fabrication, and test plan formulation effort; and an experimental-analytical effort for each subsystem) as follows:

     I.   Thrustor Analysis and Conceptual Design

    II.   Conditioner Analysis and Conceptual Design

  III.   Thrustor Design and Fabrication

   IV.   Conditioner Design and Fabrication

    V.   Thrustor Evaluation Tests

   VI.   Conditioner Evaluation Tests

This third quarterly report covers the period from 1 April 1966 through 1 July 1966.

The first two tasks have been completed.

The first portion of Task III was completed with the fabrication of the hardware required for the initial Task V experimental effort. Task V was initiated and several experimental runs accomplished. The Task VI effort was in support of the formulation of a test plan and definition of hardware designs.

Briefly summarizing, the 10-psi system has been selected for investigation. The design parameters selected include an operating mixture ratio of 2.5 corresponding to a near maximum frozen-flow specific impulse, either an in-line catalytic bed with downstream injection or an admix in-line catalyst bed, and either a radiation heat sink or regenerative chamber nozzle configuration.

The "hot-tube" heat exchanger system with H_2-O_2 combustion product feedback was chosen for the conditioner subsystem with the conditioner subsystem pneumatically decoupled from the thrustors. The basic functions of the conditioner subsystem are to (1) increase the propellant enthalpy (or temperature) above a critical value associated with freezing of the oxygen in the catalyst bed, and (2) provide a sufficiently reproducible propellant thermodynamic state for positive flow control. The approach taken in this program has been to utilize the combustion energy of the feedback O_2-H_2 stream to provide the requisite energy.

The thrustor effort was directed in two primary directions: (1) an analytical model of the thrustor was developed, incorporated in a computer program and operating characteristics determined, and (2) the experimental thrustor studies were initiated. The thrustor simulation computer program was used to evaluate the pneumatic and thermal transient responses expected in the experimental hardware and in a flight-type design. Accompanying this effort was an evaluation of the transient mixture ratio variations during start-up and shutdown. Additionally, typical pulse mode operation was examined on an initial basis. Finally, the effects of accumulator temperature and pressure perturbations on thrust and catalyst bed temperature were evaluated. The

2

sensitivity of the operating characteristics to the temperature and pressure perturbations was examined for various injector pressure drops, catalyst bed pressure drops, and feed pressure levels. The results show a ±20 R temperature band and a ±0.5 psia pressure band as a probable operating limit.

The conditioner effort was concentrated on the analysis and design of the subsystem and the components. Two aspects of the subsystem analysis were included (consideration of control system alternatives and description of the physics of the system for inclusion in a system simulation). Consideration of the control system alternatives was based on the pressure deadband requirement determined in the thrustor effort. Both pressure equalizing devices, such as bellows, and pressure regulating devices, such as regulators and follower valves, were considered. The remaining alternative is enlarging the accumulators to provide increased surge capacity. Detailed heat and material balances on the proposed experimental system were accomplished. These are to serve as the design bases for the individual components.

THRUSTOR

During the last quarter, emphasis on the thrustor effort was directed toward commencement of the experimental program, completing the thrustor modeling, and analytical studies utilizing the computer model.

EXPERIMENTAL EFFORT

Three experiments were performed during this quarter. The primary goal of these experiments was to determine the adequacy of the initial injector design in terms of mixing and to determine the necessity for utilizing a diffusion bed. All three experiments were run with a six-element, 4-on-1 (fuel-on-oxidizer) injector.

The first experiment was of approximately 16 seconds duration and resulted in damage to the catalyst bed and attendant screens. The mixture ratio was determined to be excessive (> 1.5) and in addition, there was evidence of flashback indicating a lack of homogeneity in mixing. This was determined by visual inspection of the hardware in the posttest condition, noting the similarity of burned areas in the bed, and the position of the injector elements. In addition, a high temperature was measured in the mixing section.

Steps taken to correct the situation were: (1) the inclusion of a diffusion bed made up of copper shot immediately upstream of the catalyst bed, and (2) the addition of a diffusion plate in the hydrogen manifold immediately upstream of the injector to circumvent a hydrogen ramming-starvation effect across the injector manifold, thereby retarding mixing. The copper bed is physically 3.0 inches in diameter and 0.5 inch in length.

The second experiment was run with the same injector and the above mentioned additions for a duration of approximately 14 seconds. The temperatures indicated within the catalyst bed that the mixture ratio was high (~ 1.5),

but to a lesser degree than before. Visual examination of the hardware in place, showed no signs of poor mixing or unsymmetrical hot areas. The thermocouples also indicated continuity, (they did not after the first run) and therefore the hardware was adjudged to be fit for a second run.

The third experiment was initiated after the oxidizer mass flowrate was set at a lower value. The temperature during this experiment also indicated that the run mixture ratio was slightly higher than the desired value of 1.0. However, the temperature obtained was significantly lower than on the previous run. The hardware was again visually inspected and it was determined that no hardware damage had occurred.

The data obtained during these runs are being reduced. The results of the tests will also be compared with those predicted from the computer program model. Recommendations based on the data, if any, regarding the thrustor configuration will be incorporated prior to the next experiment. Adjustments in the facility flow systems to correct the mixture ratio problem are being made prior to the next experimental effort.

SIMULATED THRUSTOR MODEL STUDIES

The mathematical modeling for the thrustor has been discussed elsewhere (Ref. 1). Once the computer model became operational, the first step was to prepare a thrustor computer program (Table I*) aimed specifically at gaining a basic insight into: (1) thrustor pneumatic and thermal response, (2) problems such as start-up and shutdown transient mixture ratio variations, (3) pulse-mode analysis, and (4) definition of accumulator operating limits.

First it is worthwhile to more explicitly state some of the initial pertinent assumptions and indicate further improvements to the model. The

─────────────────

*Tables and figures follow the text.

6

chief initial assumption was that complete combustion occurs at the entrance to the bed, so that the bed, which has been divided into five equal segments, acts as a passive mass which absorbs heat. As the gas passes through each segment it is assumed to come into thermal equilibrium with the mass. Thus, a temperature gradient is imposed across the bed which approximates experimental results provided the bed length is much longer than the minimum required to bring the gas to the auto-ignition temperature. The minimum length is estimated from previous work (Ref. 2, page 86) to be very small, approximately 0.02 inch for a 3-inch diameter.

In actuality, the temperature rise across an optimum length approaches a linear rise to the final combustion temperature. Any additional catalyst mass past this optimum quantity then acts as a passive mass as previously discussed. Since all the catalyst bed is assumed completely passive in the present model, the thermal and pneumatic responses given by the computer model are conservative, i.e., too slow. A better mathematical model was later developed which relaxed the assumption of complete combustion at the upstream face and forced a specified temperature rise across a given length. An example output of this model is given later in the definition of accumulator operating limits.

Another initial approximation was the method by which catalyst bed pressure drop is calculated. The program treats the bed as if it were an orifice sized for a specified steady state pressure drop. A good approximation to the steady-state pressure drop can be read from the 10-psia curve of Fig. 27, page 145, Ref. 3, which is traceable to an experimental data point.

An alternative to this method of treating the pressure drop across the catalyst bed is to use the Ergun Equation (Ref. 3). Unfortunately, it has been found that this equation is extremely sensitive to the ϵ, void fraction; thus it is concluded that the present approach is better than a more theoretical approach. Appendix A shows that the Ergun Equation can

be reduced to an orifice-type equation if one neglects the laminar friction term which is generally less than 25 percent of the total pressure drop.

The analysis presented in Appendix A shows the catalyst bed to act as a series of orifices, the number of which is given by L/D_p. It is further shown that the average density of the gas in the bed, as determined from the temperature and pressure profiles within the bed, must be used. This improvement was incorporated into the computer model. As more experimental data become available, better methods to correlate pressure drop can be found and included in the thrustor model.

Thrustor Pneumatic and Thermal Response

Typical steady-state start-up pneumatic and thermal responses for a 0.525-inch catalyst bed are presented in Fig. 1, 2, and 3. Figure 1 shows the response of chamber pressure, mixer section pressure, inlet pressures, thrust, and inlet valve orifice area as a function of time.

Figure 2 depicts the inlet temperatures to the catalyst bed, T_o, and the temperatures of the five segments of the bed. Each bed segment corresponds to a given length increment. For example, the first curve represents a bed of about two pellets, the second, four pellets thick, etc. For the case of full flow, the last segment also represents the combustion chamber temperature. Instantaneous flowrates and chamber mixture ratio as functions of time are shown in Fig. 3.

To understand how the thrustor performs all three charts must be integrated simultaneously rather than individually. Looking first at the lefthand side of the charts, it can be seen that it takes approximately 75 milliseconds for the temperature of the last node to start to rise. During this time period, the instantaneous chamber pressure, thrust, specific impulse, and flowrates reach steady-state values indicative of cold flow.

8

Then as the temperature of the last node of the catalyst bed increases, chamber pressure, thrust, and specific impulse exponentially approach their steady-state values. Since the throat will allow a higher flowrate at low temperature, or high density, than at operating temperature, the flowrates decrease to their steady-state values.

The same set of curves were prepared for downstream injection (DSI) of oxygen at 1500 R. At this point there is a distinct discontinuity in all curves to their steady-state values except the catalyst bed temperatures, because instantaneous combustion of O_2 was assumed.

To gain some insight into the differences of full flow and DSI of O_2, the computer results were compared. Of particular interest is the bed temperature response. Since the temperature driving force is higher for full flow than for DSI, the full-flow bed reaches the auto-ignition quicker than the DSI bed. However, the overall thermal response is identical, approximately 750 milliseconds. An example of DSI with the latest computer model is given in the worst case section.

Transient Mixture Ratio Variations

Figures 4 through 6 illustrate the fuel-rich mixture ratio (MR) variation which occurs on start-up. Although not shown, the reverse is true on shutdown. The cause of this undesirable variation is the difference in the rate of filling of the O_2 and H_2 pre-injector volumes must be the same as the ratio of the molar flowrate of propellants $\dfrac{V_{H_2}}{V_{O_2}} = \dfrac{1}{MR} \dfrac{MW_{O_2}}{MW_{H_2}} = 6.4$. The example shown is for the geometry (volume ratio of 1.25) of the present experimental thrustor. The hydrogen chamber fills and empties much more rapidly on start-up and shutdown than the oxygen chamber, thus causing the MR to be fuel-rich on start-up and oxidizer-rich on shutdown.

9

Two solutions to this problem were investigated. One involved valve sequencing. Even with a 100-millisecond O_2 closure lead, it was concluded that the mixture ratio would still go oxidizer-rich on shutdown. It was further concluded that valve sequencing would not be satisfactory for pulse-mode operation.

The only feasible solution to this problem is to readjust pre-injector volumes to make them equal the molal flowrates. This correction must be made before the thrustor can be safely operated in the pulse-mode fashion.

Another undesirable feature of the pre-injector volume is that the residual propellants must pass through the thrustor after shutdown, consequently putting a "tail" on the performance curves. Thus, there is a great deal of incentive to keep the pre-injector volumes small and in the correct volume ratios.

Pulse-Mode Analysis

Studies of the pulse-mode operation have been made, and it has been concluded that the present experimental thrustor will operate satisfactorily in the pulse-mode fashion provided the restrictions in the preceding paragraphs are met. An example of a typical pulse is given in the worst case definition section of this report.

A matrix of experimental runs was carefully planned so that the computer model could be used for interpolation and extrapolation. Before this could be done it was necessary to define rather explicitly and experimentally measure such computer input data as volumes, areas, catalyst bed properties such as node temperatures, catalyst weight, and pressure drop. Then a quantitative comparison of computer calculated thermal, pneumatic, and flowrate responses can be made with the respective experimental responses. Acceptable comparison limits are currently being defined. After successful quantitative checkout, the final thrustor performance interpolation and extrapolation can commence.

Effect of Feed Perturbations on
Thrustor Performance

The thrustor performance variation (ΔF) and the fluctuation in catalyst
bed temperature are a function of changes in propellant inlet pressure
and temperature from nominal design. Variations in the propellant inlet
condition are governed by pressure and temperature design tolerances of
the conditioning system.

Nominal design operation of the conditioner system calls for on-off oper-
ation depending on accumulator pressure; on at 16.0 psia, off at 17.5 psia.
For steady-state, thrustor demand with approximate accumulator volume of
1200 cu in. for H_2 and 250 cu in. for O_2 the conditioner system must operate
with frequencies of about 10 to 15 cps or fire about every 50 to 100
milliseconds.

It is desirable to know what effect this perturbation will have on thrustor
performance. Worst case conditions for this oscillation results when the
highest O_2 density couples with the lowest H_2 density or vice versa. More
specifically, the worst case is defined as one thrustor inlet set at 17.5
psia (the accumulator relief pressure), and the other inlet set at the
given minimum pressure. At this condition the inlet temperatures were set
such that the lower temperature was always matched with the higher pressure.
For example, if the minimum pressure is 15 psia at the oxygen inlet, and
the temperature band is ±20 R, the inlet conditions would be 15 psia and
220 R at the oxidizer inlet and 17.5 psia and 180 R at the hydrogen inlet.

These steady-state pressure and temperature perturbations were fed into
the thrustor computer model and the changes in catalyst bed temperature
and thrust were noted.

The change in catalyst bed temperature from nominal design for DSI at 2000 R
vs variation is plotted in Fig. 7. The inlet pressure from nominal (17 or
20 psia) with catalyst bed pressure drop (ΔP_{cat}), the second inlet pressure

the temperature deadband (± 20 R), and the nominal design pressure are parameters. For example, for the upper middle two curves the parameters have been set at:

1. $\Delta P_{cat} = 2.0$

2. O_2 inlet pressure = 17.5 psia for solid and 20.5 for dashed lines

3. O_2 inlet temperature = 180 R

4. H_2 inlet temperature = 220 R.

As the H_2 inlet pressure is reduced from nominal the H_2 flow decreases causing the mixture ratio and consequently the bed temperature to increase. The extreme lefthand point considered the worst oxidizer-rich case since the highest O_2 pressure and lowest O_2 temperature are coupled with the lowest H_2 pressure and highest H_2 temperature, thus giving the highest MR change.

For the bottom set of curves the temperature deadband has been reversed and the H_2 inlet pressure has been set at 17.5 psia while the O_2 pressure has been varied, thus illustrating the fuel-rich case.

It can be concluded from Fig. 7 that catalyst bed pressure drop has the most pronounced effect on catalyst bed combustion temperature. As the nominal design pressure drop across the catalyst bed is increased, the allowable nominal pressure drop across the injector face decreases. For example, when the ΔP_{cat} is 4.0, the nominal pressure drop across the injector face is 3.0 psi. When the hydrogen inlet pressure is decreased to 15.0 psia the hydrogen ΔP across the injector face is decreased to about 1 psi or by a factor of 3. Thus, the net effect of a large ΔP_{cat} is to choke off the flow of the lowest pressure propellant and thus cause large variations in the catalyst bed combustion temperature.

The net effect of increasing the nominal pressure to 20 psia is to damp out the shift in combustion temperature with ΔP_{cat}.

Calculations (Appendix B) were made for the case of $\Delta P_{cat} = 0$ for a nominal pressure of 17.0. The computer curves seem to approach this limit as ΔP_{cat} is lowered, thus the results are deemed in agreement.

The effect of temperature deadband of ±20 R can be isolated from inlet pressure variations by noting the righthand point where propellant pressures are equal. It can be concluded that shifts in propellant inlet temperatures are less important than shifts in propellant inlet pressure.

Figure 8 shows how the thrust varies as a function of the same inlet perturbation and parameters as used in the previous example.

When the catalyst bed temperature decreases 500 R from nominal (arbitrarily selected) the O_2 bypass valve will close. This, in turn, causes a discontinuity in the lower fuel-rich thrust curves of Fig. 8.

The thrust variation curves for the oxidizer-rich case (upper curves) appear to be relatively insensitive to hydrogen inlet pressure. These curves are displaced a horizontal distance of about 0.05 which indicated that the temperature deadband of ±20 R is the controlling factor. The reverse is true for the lower curves.

Changes in catalyst bed temperature for full flow (nominal bed temperature 4000 R) as a function of inlet propellant perturbations (Fig. 9) have not been fully investigated. But, the results are similar to those shown in Fig. 8 for the DSI case with the exception that the swings in temperature for a given perturbation are larger for full flow. Equation 4 in Appendix B

$$MR = \frac{P_{O_2\ inlet}}{P_{H_2\ inlet}} \sqrt{\frac{T\ inlet\ H_2}{T\ inlet\ O_2}} \ (MR\ nominal)$$

shows that a given inlet perturbation is multiplied by the original mixture ratio. Thus, the larger the nominal mixture ratio, the larger the swings in catalyst bed temperature.

It is also shown in Appendix B that the thrust variation should be the same for DSI and full flow for the special case of $\Delta P_{cat} = 0$. This results from the fact that the change in mixture ratio in the combustion chamber for both cases is identical.

In actuality, the accumulator pressure cycles within a deadband with a frequency near that of the pulse frequency. This dynamic perturbation is discussed in the following section for comparison with the aforementioned conclusions.

Worst Case Definition. It was noted that the previous definition of the worst case situation assumed the highest O_2 pressure (17.5 psia) and the lowest O_2 temperature (180 R) are coupled with the lowest H_2 pressure (15.0 psia) and the highest H_2 temperature (270 R). This may be unduly restrictive, since the accumulator pressure cycles within a deadband with a frequency near that of the pulse frequency and is not constant as previously assumed. A dynamic accumulator perturbation was studied using the most recent version of the computer thrustor model which has a sinusoidal accumulator pressure generator $\left(Po + \frac{\Delta P}{2} \sin 2\pi ft \right)$ and provisions for inserting any desired temperature gradient (or gradient in fraction of reacted propellant) across the bed. The particular input data as noted in Fig. 1 through 3 was the same as for the previous worst oxidizer-rich case so that a direct comparison could be made with the original results to check the original definition.

Figures 4 through 6 show the pneumatic, thermal, and weight flowrates for a typical experimental thrustor being pulsed for 150 milliseconds near operating temperature. The inlet pressure frequencies are typical for accumulator designs presently being considered.

Simultaneous inspection of the three plots reveals that:

1. The pressure in the mixing zone and, less strongly, chamber pressure and thrust follow the cyclic H_2 pressure. The effect on chamber pressure and thrust results from the fact that the molal (or volumetric) flowrate ratio of hydrogen to oxygen at design conditions is 6.4. Thus, a 10- to 20-percent variation in O_2 flowrate has an insignificant effect on total molal flow.

2. When the propellant pressures are 180 degrees out-of-phase with P_{H_2} being a maximum, the P_{O_2} injector will be at a minimum of about 0.2 psia. Consequently, the O_2 flowrate cycles through a wide amplitude as shown in Fig. 6 . The instantaneous combustion temperature (T_0) in Fig. 5 also cycles through wide extremes.

3. The maximum increase in catalyst bed node temperatures are approximately 400 R or about one-third of the increase in combustion temperature. The increase in temperature of each node is dependent upon the assumed nominal temperature, e.g., fraction reaction and the mass represented by the node. It appears that the gradient of propellant reacted through the bed is beneficial in damping out temperature swings or spreading out the increase in combustion enthalpy release.

4. The frequency of the throat flowrate corresponds to the frequency of the O_2 weight flowrate because there is nominally 2.5 times more O_2 flowing than H_2 by weight.

When these results are compared to the original results of Fig. 2, Ref. 4, it can be concluded that the swings in catalyst bed temperature are significantly less than previously expected. This difference can be attributed to the change in the mathematical model which better describes the real case. Perturbation experiments should be considered in the thrustor task to definitely establish permissible accumulator operating limits.

Provided the definitions of worst case conditions are accepted, it can be concluded that the swings in catalyst bed temperature are too high, and therefore, some type of pressure and/or temperature equalizing devices must be installed on the accumulators. Pressure regulators were originally considered and discarded in favor of a lighter more reliable pressure relief valve. However, because of the new results, pressure regulators were considered as a method of eliminating catalyst bed temperature fluctuations. The feasibility of bellows pressure equalizing device on the accumulators was also investigated. These results are presented in the Conditioner Design Section.

The prime emphasis of the conditioner effort (Tasks IV and VI) has been on detailed analysis of the individual conditioner components, design of the components, system analyses and modeling, and consideration of control system alternatives.

OVERALL CONDITIONER HEAT AND MATERIAL BALANCES AND SIZING CRITERIA

The conditioner system can be considered as a black box which must convert propellants from their inlet thermodynamic condition to a superheated gaseous state at 200 ±20 R and 17 ±0.5 psia. It is readily seen that the maximum heat load occurs when saturated liquid must be vaporized and thus the conditioning components selected in Task II, Gas Generators and Hot-Tube Heat Exchangers, must be sized for this case. Overall heat and material balances have been made for the case of saturated liquid vaporization with the gas generators operating at 2500 R, and are presented in Tables 2 through 4. Balances are also shown for the case of saturated vapor propellants to illustrate the reduction of heat loads and flows.

The efficiency with which the black box operates, as measured by the percent of total flow diverted to the gas generators, is an important variable, since the system impulse is determined by the thrustor plus gas generator flows. The flow to the gas generators can be reduced by increasing the mixture ratio as shown in Table 2, but unfortunately, for a single-stage combustor, the system reliability decreases rapidly because of the possibility of catalyst bed burnout and metal failure. Because of this factor, a gas generator mixture ratio of 1 has been selected for experimental investigation. A method of increasing the mixture ratio to 2.5 is currently being investigated in the experimental thrustor program, Task V. This information will demonstrate the feasibility of high mixture ratio operation of the gas generators.

An alternative method of raising the efficiency is the staged reaction concept. In this concept, the reaction is carried out in a series of catalyst beds with additional oxygen injected just upstream of each bed. The requisite amount of heat transfer is allowed between each stage. The advantages of this system include low local temperatures which accompanies the increased efficiency.

The minimum instrumentation required for a material balance around the system is: (1) measurement of each thrustor flowrate, and (2) measurement of the total flow of each propellant to the gas generators. The conditioner efficiency is then given by

$$\text{Cond } (\eta) = \frac{\left(w_{O_2 T} + w_{H_2 T}\right) 100}{\left(\dot{w}_{O_2 gg} + \dot{w}_{H_2 gg}\right) + \left(\dot{w}_{O_2 T} + \dot{w}_{H_2 T}\right)} \quad (1)$$

The best location for flow measurement in the experimental program appears to be downstream of the accumulator where the quality, pressure, and temperature are being controlled.

DESIGN OF THE INDIVIDUAL COMPONENTS

Gas Generators

From the maximum heat load requirements of the conditioning system, as presented in Table 2, the maximum flowrates to the individual gas generators can be calculated as shown in Tables 3 and 4. The actual sizing of the gas generators depends upon optimization with respect to the following factors (Ref. 3):

1. Mixing volume velocities sufficiently high to prevent flashback

2. Catalyst bed length sufficiently long for ignition

3. Catalyst bed pressure drop low consistent with total pressure head

Past experience (Ref. 5) has also shown the 4-on-1 injector to be superior for mixing. Using these criteria the two gas generators (Fig. 10 and 11) were designed. The pertinent parameters are given in Table 5.

The pre-injector volume ratio has been set at the ratio of the filling rates, (16.0) to eliminate the possibility of transient mixture ratio variations. In reality, it should not be difficult to satisfy this volume ratio restriction since the injectors shown in Fig. 10 and 11 minimize the O_2 volume and maximized the H_2 volume.

Information feedback from the thrustor studies will be used to optimize the internal gas generator design, although it is recognized that optimum performance here is not as important as reliability.

The throat areas presented in Table 5 are sized for sonic flow. It is thought to be highly desirable to have a sonic orifice between the gas generator and the heat exchanger coil to minimize the effect of downstream perturbations on gas generator behavior.

Since the purpose of the gas generator is to deliver a fixed amount of hot gas at a specified temperature and pressure to the heat exchanger, the minimum amount of instrumentation is inlet flow measurements, as discussed previously, and coil inlet temperature and pressure measurements.

Heat Exchanger

In Task II four conditioner designs were evaluated. From a concept comparison (Table 12, Ref. 3) it was determined that the hot-tube heat exchanger concept appeared to be the most promising and thus it was selected for a detail design, Task IV, and experimental evaluation, Task VI.

Detailed O_2 and H_2 heat exchanger and gas generator designs were proposed in Ref. 1, Fig. 4 through 7. The sizing technique has been detailed in Ref. 3, pages 9 to 12 and Appendix A. The heat exchanger design evaluations can be traced through the quarterly reports to the proposed designs which features:

1. Low propellant pressure drop

2. High thermal response

3. Minimization of heat leak by surrounding the hot tube with the coolant

4. Simplicity of construction

Thus, the basic designs as proposed in Ref. 3 have been preserved.

In the interest of reliability it was decided to reduce the gas generator operating temperature from 2500 R to 2000 R. Thus, it was necessary to resize the heat exchanger using the original methods (Ref. 1) to take into account the decrease in driving temperature and the increase in hot-gas flowrate. These results are presented in Tables 3 and 4 along with the original results.

The basic equation used to size the typical heat exchanger shown in Fig. 4, Ref. 1 is the familiar equation

$$q = U \, A \, \Delta T_{lm} \tag{2}$$

where

$$\frac{1}{U} = \frac{1}{h_g} + \frac{1}{h_l} \tag{3}$$

Heat transfer coefficients are given in Table 6. Steady-state tempera-
ture profiles through the heat exchanger are presented in Fig. 12. The
tube wall temperature was calculated from

$$(T_g - T_w) = h_1 (T_w - T_g) \tag{4}$$

Figure 12 shows that there is considerable difference between the O_2 and
H_2 heat exchangers. First, the H_2 tube wall tempetature is considerably
lower than for O_2 because of the much higher heat transfer coefficient
for H_2. Secondly, over 90 percent of the O_2 HX area is required for the
vaporization of O_2, whereas only 30 percent is required for the H_2 heat
exchanger. This information should prove helpful in instrumenting the
heat exchanger if flow instability becomes a problem.

Liquid, gas, and tube wall temperatures will be measured at the same loca-
tion so that Eq. 4 can be applied to determine the ratio of heat transfer
coefficients.

It is possible to make exacting calormetric measurements around the heat
exchanger only with a great deal of effort. For example, the flows must
be carefully measured, the heat leak accurately calibrated, the inlet
quality of the propellant controlled, and the thermodynamic properties
of both propellant and hot gas accurately known. Therefore, at this
time it is considered feasible to measure only the temperature profiles
through the heat exchanger and to thus make pseudo-calormetric measurements.

Accumulators

An accumulator is used to decouple the conditioner system from the thrustor.
To accomplish this the accumulator must be sized to damp   out (1) pressure
perturbations caused by the main propellant valve delay (the electrical and

mechanical valve delays), and (2) pressure and temperature perturbations produced by the heat exchanger. Of these perturbations, the former is the most predictable through a material balance:

input - output = accumulation

$$0 - \dot{w}_T = \frac{V}{TR} \frac{dP_{acc}}{d\theta} \qquad (5)$$

where

$$\dot{w}_T = \dot{w}_{T\ nom} \left[\frac{(2g\ \rho_T\ \Delta P_{inj})}{(2g\ \rho_{T_{nom}}\ \Delta P_{nom})} \right]^{1/2} \simeq \dot{w}_{T\ nom} \sqrt{\frac{P_{Acc}}{P_{nom}}} \qquad (5a)$$

Integration gives:

$$-\left[\dot{w}_{T\ nom} \frac{TR}{V} \right]\theta = 2\sqrt{P_o} \left[P_f^{1/2} - P_o^{1/2} \right] \qquad (6)$$

A plot of accumulator pressure vs valve time delay with accumulator volume as a parameter is given in Fig. 13. Worst case accumulator limits presented in Ref. 6 showed that it is desirable to hold the accumulator pressures to within about ±0.5 psi of each other. If this ΔP is used with a main propellant valve delay of 0.050 seconds, accumulator volumes of 2720 sq in. and 424 sq in. for H_2 and O_2, respectively, can be calculated.

At the present time little is known about boiling instability which could conceivably cause large pressure and temperature perturbations in the inlet . stream to the accumulator. An estimate of the thermal response to steady-state inlet tempetature perturbations can be obtained by considering a heat balance around the accumulator.

$$\dot{w}\ C_p\ T_{in} - \dot{w}\ C_p\ T_{acc} = M\ C_p\ \frac{dT_{acc}}{d\theta} \qquad (7)$$

or

$$\frac{\dot{w}}{M}\ \theta = \ln \left[\frac{T_{in} - T_{f\ acc}}{T_{in} - 200} \right] \qquad (8)$$

22

The time for the accumulator tempetature to reach 200 R for T_{in} of 100 and 500 R can be computed to be 41 and 94 milliseconds, respectively, for the volumes sized in the previous paragraphs. This illustrates the importance of selecting the correct hot-tube temperature set point.

A cursory heat transfer analysis of the temperature equalizing advantage of placing the O_2 accumulator inside the H_2 accumulator was made assuming concentric cylindrical containers 2 feet in length. Under steady-state conditions there is a negligible equalizing effect for a 40 R temperature difference. A convective analysis for static no-flow conditions indicates that the response is somewhat better although still small. It was concluded that if a temperature equalizing device is necessary one should design a low-pressure drop combination accumulator-heat exchanger similar to the design proposed in Fig. 4 (Ref. 1).

It is proposed to make both accumulators about 2 feet long with diameters of 13 and 5 inches for H_2 and O_2, respectively. Since a good portion of the system weight and volume is represented by the accumulators, an important part of the experiment will be to minimize the accumulator size.

Minimum instrumentation required for the accumulators is temperature and pressure measurements at the inlet and outlet.

SYSTEM ANALYSIS

Conditioner system computer modeling, built around Fig. 14 was briefly discussed elsewhere (Ref. 1). Reference should be made to this material for a discussion of the basic equations and techniques employed. The purpose here is to discuss the actual input data and to present the analysis of the initial system dynamics.

An example of typical computer input data is given in Table 7 for the special case of saturated O_2 vapor propellant feed to the O_2 conditioner. Important input data from Table 7 are:

1. Control points and deadbands

    a. The accumulator set point pressure is 17.0 ±0.5 psi. This control circuit operates the main propellant valve.

    b. The accumulator set point temperature is 200 ±5.0 R. This control circuit turns the gas generator on or off when the main propellant tank valve is open.

    c. The tube wall set point temperature is 400 ±120 R. This control circuit operates only when the main propellant valve is closed and is designed to keep the tube hot during the coast mode.

2. Main propellant valve delay is 0.020 second.

3. Accumulator volume is 250 cu in.

4. Thrustor duty cycle delay, frequency, and duration is 0.60 second, 1 cps, and 100 percent, respectively.

5. Thermal resistance within the heat exchanger and the tube wall heat capacity as shown in Table 3.

These values were arbitrarily selected but are typical of the present conditioning system.

Figures 15 through 18 show the valve, temperature, pressure, and weight responses for this case. The sequence of operation is approximately:

1. Initial wall temperature is low causing the gas generator to turn on (Fig. 15) thus causing the wall temperature to increase.

2. Low accumulator pressure signals main propellant valve to open (Fig. 15) causing:

   a. Inlet pressure to heat exchanger (Fig. 17) buildup

   b. Flow to surge into heat exchanger (Fig. 18)

   c. Accumulator temperature to drop (Fig. 16) because of the low wall temperature

3. When the accumulator pressure reaches 17.5, a signal is sent to the main propellant valve to close. A 20-millisecond delay causes the pressure to overshoot.

4. Excess pressure is vented by the relief valve.

5. The process is essentially repeated again when the thrustor valve opens again at 0.6 second.

It is of interest to note that the gas generator does not turn off when the main propellant valve closes. Inspection of the tube wall control loop set point and deadband reveals that the gas generator will not close until a wall temperature of 520 R is reached.

Another control loop, not previously discussed, causes the oxidizer flow to the gas generator to shut off (Fig. 15) when the catalyst temperature reaches 2000 R as shown in Fig. 16. This valve cycling causes pressure and temperature perturbations as shown in Fig. 16 and 17.

Under normal operation with saturated vapor feed, the gas generator must cycle on and off because it has been sized to supply enough heat to vaporize liquid. However, during the start-up period the tube wall is absorbing enough heat to keep the gas generator on.

Computer runs similar to those presented in the preceding paragraphs for saturated O_2 vapor were made for (1) saturated O_2 liquid, (2) saturated H_2

vapor, and (3) saturated H_2 liquid for both pulse and steady thrustor demand. The main differences and conclusion are:

1. A large amount of liquid O_2 surges into the heat exchanger when the main propellant valve is opened because the propellant valve must be sized for saturated O_2 vapor flow which has a density several hundred times less than that for saturated liquid. The net effect of this phenomenon is to cause the main valve to cycle on and off, although there is a steady flow demand by the thrustor.

2. There is not a great difference between H_2 vapor and liquid flow into the heat exchanger because of the small density difference between H_2 vapor and liquid. This factor can probably be used to advantage in the control circuit. For example, the bang-bang pressure controller should possibly be put on the H_2 side and the variable orifice follower on the O_2 side.

3. In one case the $\dot{w}_{O_2}$ gas generator and $\dot{w}_{H_2}$ gas generator rose to only one-half of their nominal design values of 0.0020 lb/sec. The trouble was traced to the hot-gas dump pressure which was approximately twice its normal value. It was concluded that the hot-gas orifice has been missized. In this particular situation flashback to the injector face might have occurred.

PRELIMINARY EVALUATION OF BELLOWS AND
BLADDERS FOR PRESSURE EQUALIZATION

Because of the need to reduce or control the pressure difference between the inlet propellant from each accumulator, the feasibility of separating

the containers with a diaphragm or bellows was investigated. A cursory literature survey revealed that the Beech Aircraft Corporation has investigated the use of expulsion bladders for cryogenic fluids (Ref. 7 and 8). Since any one of three limitations listed by Beech Aircraft: incompatibility with LOX, low cycle life, and permeability, could have catastrophic results, bladders at this time were considered not feasible.

The feasbility of integrating a bellows O_2 accumulator into the larger H_2 accumulator has passed through several concept evaluation stages:

1. The bellows would have to be 7.5 inches long with a 6.5 inch ID and would have to be capable of expanding 6.6 inches and contracting 1.1 inches at a frequency of 10 to 15 cps. A spring constant of 2.5 lbf/in. or less would be desirable.

2. A cursory mathematical description of the bellows dynamics action was programmed on the digital computer using the Midas technique, Ref. 9 and 10. It appears that the mass and spring constants necessary to give a rapid response are compatible with present-day manufacture.

3. Correspondence and discussions with vendors.

A local representative of the Belfab Corporation (which has considerable experience in designing bellows-type expulsion bladders) was given the preliminary sizing requirements and reported that a bellows with the following parameters could be built:

OD = 9 inches; ID = 7.2 inches; spring constant (K) = 5 lbf/in.

Free length $\approx$ 6 inches; Δ L Maximum contraction = 4.17 inches; Δ L maximum extension = 9.25 inches

ΔP_{max} = 3 psi; area mean effective = 51.5 sq in.; Δ V displaced = 219 cu in.

ΔV_{comp} = 215 cu in.; 347 stainless steel, cycle life 30,000; 3.25 pounds; 200 R

Generally it was concluded that cycle-life failure would be the chief shortcoming although the 30,000 cycle life reported by Belfab is much greater than that which might be expected from past experience (Ref. 11 and 12). However, the cycle life is sufficiently long so that the mathematical model should be improved to represent reality and a detailed application study should be made.

CONTROL SYSTEM CONCEPTS FOR THE CONDITIONER

Several different schemes and initial evaluations other than the bellows arrangement are presented below. Most of the effort has been spent in evaluating the use and placement of a pressure regulation and equalization system to equalize the pressures delivered from each accumulator. The basic components common to each scheme includes a heat exchanger, hot-gas generator, an accumulator, and the main valve for the thrustor.

Pressure Control

Method A: No Pressure Equalizing System. This represents the initial control scheme proposed. The system concept was based on dividing the conditioner system into individual components and maximizing the performance of each component. A schematic of the system is shown in Fig. 19. The principal control loops are as follows:

1. Hot-tube temperature control in the heat exchanger--This loop controls both the hydrogen and oxygen flow to the gas generator during the coast modes of the vehicle. The tubes are kept hot to circumvent the relatively long time ($\sim$ 2 to 5 seconds) needed to heat the tubes to steady-state conditions. An automatic reset capability of the reference temperature is included to allow for variations in the quality of the propellants delivered from the main tanks. The reference point is determined prior to closing the main thrustor valve and is maintained through the coast period.

28

2. Accumulator temperature control--When the hot-tube temperature control is nullified (during thrustor operation) the accumulator temperature controls the flow of hydrogen and oxygen to the gas generator.

3. Accumulator pressure control--The accumulator pressure control causes the tank valve to open at a specified low pressure and close at the nominal accumulator pressure. If the accumulator pressure exceeds the nominal value, the pressure relief valve will open to relieve the overpressure.

Evaluation. Four valves and three principal control loops are used. A conceivable problem exists in the pressure controlling device for the accumulator. An oscillation could be established between the pressure relief valve and the tank valve although, if significant, an increase in accumulator volume will eliminate the oscillation. This oscillation could develop during the conditioning cycle, since pressure perturbations caused by liquid slugging in the heat exchanger may be present. In addition, the pressure in the fuel accumulator is not necessarily equivalent to the oxidizer accumulator pressure. Another problem is in sizing an effective orifice for the gaseous propellant tank valve. The specific volume of the propellant can vary considerably because of all-liquid to all-gas transitions as well as possible helium content in the propellant. Consequently, the flowrate of propellant delivered to the heat exchanger could vary over a large range for a fixed valve orifice area.

Method B: Pressure Regulator. A possible way to circumvent the problems that would be incurred with Method A is to use a pressure regulator in place of the main valve.

From Vehicle Tank

Overboard

Hot Gas

To Main Valve
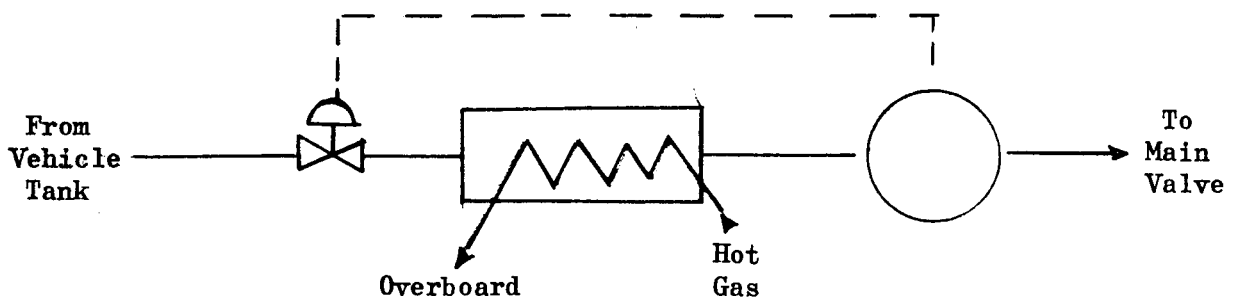
The regulator would take its reference point from the accumulator which contains propellant entirely in a gaseous state. The need for a pressure relief valve would be eliminated for control purposes, although a relief valve could be employed as a safety device. The accumulator is conservatively sized such that the regulator does not have to function for every short (~ 50 millisecond) pulse of the thrustor. The fuel-side regulator deadband would be matched with the oxidizer regulator such that the pressure differential between the accumulators would at no time exceed a set value. At this time 1 psi appears to be a reasonable deadband.

Evaluation. A difficulty could arise in this scheme during the coast mode. Even though the regulator is closed and the accumulator topped off, the gas remaining in the heat exchanger is continuously being heated by the hot tubes. The gas will affect the accumulator state by a diffusion process due to a temperature gradient and/or pressure flow. An estimate will be made of the gas temperature and pressure increase in the accumulator. The accumulator sizing is again important since the larger the reservoir, the less the effect of the heat exchanger during the coast mode. An attenuating effect evolves from keeping the heat exchanger tubes and the gas generator at an elevated temperature. This requires an intermittent flow of conditioned propellant from the accumulator even during the coast mode.

Another possible problem arises from the two-phase flow conditions in the heat exchanger which can lead to pressure drop and flowrate fluctuations through the heat exchanger. The accumulator will be sized to successfully damp the pressure fluctuations that might be encountered.

The accumulators need to be sufficiently large to provide time for the regulator to respond from a fully closed (locked up) position to an open position. This problem might be eliminated by not having the regulators lock up. During the coast mode, the conditioned propellant would flow

back toward the main vehicle tanks. However, the line volume between the main tanks and the regulators should be large enough to account for the increased propellant temperature from the heat exchanger.

Method C: Pressure Regulator Between the Heat Exchanger and Accumulator.
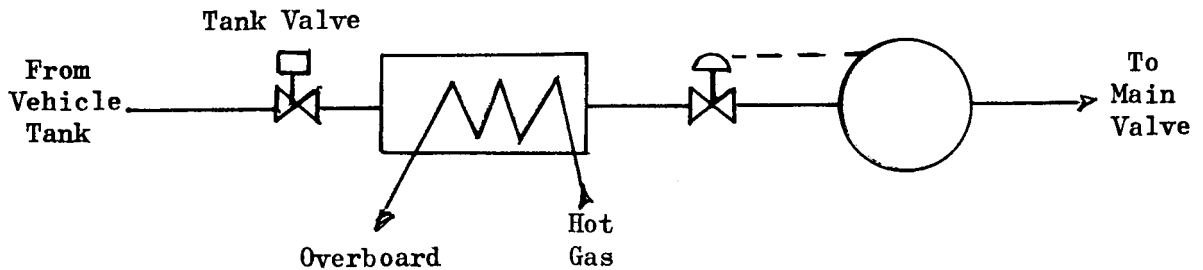
If the pressure regulator never locks up the response of the system is increased and the need for an accumulator might be eliminated. In practice, however, a small accumulator will be necessary. Placing the regulator downstream of the heat exchanger might require either a tank valve or a check valve to prevent back flow from the heat exchanger during the coast mode. If the tank valve is necessary, a danger exists in overpressurizing the gas in the heat exchanger during the coast mode. However, a demand will be placed on the accumulator during the coast period (to maintain heat exchanger tube temperature), thus attenuating the overpressure condition.

Method D: Pressure Regulator Plus Follower.
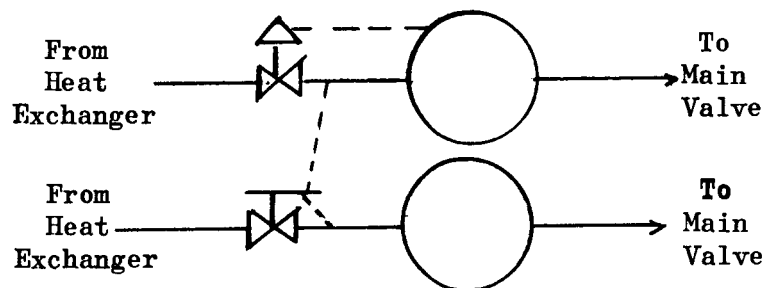
Instead of using a pressure regulator for each side, a follower valve can be placed on one side. This would tend to equalize the pressures to a greater extent, since the possible error in a two regulator system would be the sum of the tolerances. In addition, the weight of the system would be decreased since the follower is not as elaborate a device as a regulator. The position of the follower in the system is a function of the same criteria that applies to the regulators.

Temperature Control

In addition to a pressure control system, a temperature control is needed. Three distinct phases can be investigated while determining what type of temperature control system to use. They are: (1) what type of temperature sensor to use, (2) where to place it, and (3) what should it control.

The temperature sensing devices should give a relatively large current or electromotive force (emf) delta output for a small change in temperature in the cryogenic range. A device that appears to meet these qualification is a thermister. The placement of the sensor should be upstream of the main thrustor valve since an erroneous temperature would be after the fact. The sensor, however, should probably not be placed either in or immediately downstream of the heat exchanger due to the possibility of local temperature and pressure fluctuations which may drive the control system unstable.

The temperature control will open or close the gas generator valves that provide the hot fluid. No provision is made for cooling the gas in the accumulator other than radiation losses. It is expected that the control loop will sense a slug of overheated gas entering the accumulator and shut off the gas generator valves fast enough for the accumulator volume to assimilate the slug without exceeding the mean temperature deadband. The

ideal situation is to use a bipropellant valve for the gas generator so that both propellants enter the mixing volume simultaneously. The volumes will be sized such that the gas generator will not go oxidizer-rich during either the start or stop transients. The experimental program will not use a bipropellant valve since one is not readily available. Instead, two relatively fast response ($\sim$ 50 milliseconds) valves will be matched and the electrical signal given at the same time.

FUTURE EFFORTS

The thrustor effort (Tasks III and V) will be directed towards accomplishing the experimental program. This includes effort to more completely define catalyst bed design criteria and to determine combustion volume requirements for downstream oxidizer injection. Following these experiments a design configuration will be selected for the remainder of the program based on the confirmed catalyst bed design criteria and downstream combustion volume requirements determined experimentally. A calorimeter chamber will be used to determine heat fluxes and heat transfer coefficient by the transient temperature technique. The altitude performance and pulse-mode characterization task will be initiated at the close of the reporting period.

The conditioner efforts (Tasks IV and VI) will initially concentrate on the fabrication of the necessary hardware components and the buildup of a test stand. This is to be followed by component testing on the gas generators, the heat exchangers, and the accumulators. Following this effort will be the experimental mating of the components and the imposition of the requisite control systems. The successful completion of this effort will enable integrated system testing in the following report period.

NOMENCLATURE

A	=	area, constant
B	=	constant
C	=	constant
D	=	diameter, constant
F	=	thrust
G	=	superficial mass flux
K	=	spring constant
L	=	length
M	=	mass
P	=	pressure
R	=	gas constant
T	=	temperature
U	=	overall heat transfer coefficient
V	=	volume
W	=	weight
X	=	fraction reacted
HX	=	heat exchanger
MW	=	molecular weight
MR	=	mixture ratio
g	=	gravitational constant
h	=	heat transfer coefficient
k	=	heat capacity ratio
q	=	heat rate
w	=	weight

SUBSCRIPTS AND SUPERSCRIPTS

$\cdot$	=	time derivative
p	=	pellet
cat	=	catalyst bed
T	=	thrustor
gg	=	gas generator
acc	=	accumulator
f	=	final
o	=	initial, superficial
max	=	maximum
comp	=	compressed
ss	=	steady state
c	=	chamber
lm	=	log mean
g	=	gas
l	=	liquid
w	=	wall
in	=	inlet
nom	=	nominal
F.F.	=	full flow

GREEK SYMBOLS

Δ	=	delta
ρ	=	density
θ	=	time
ϵ	=	porosity
μ	=	viscosity
α	=	fraction reacted

OTHER SYMBOLS

O_2 = oxygen

H_2 = hydrogen

> = greater than

~ = approximately

$d/d\theta$ = time derivative

C_p = heat capacity

ln = natural log

emf = electromotive force

REFERENCES

1. R-6342-3, Evaluation and Demonstration of the Use of Cryogenic Propellants (O_2-H_2) for Reaction Control Systems, Third Quarterly Report, Rocketdyne, a Division of North American Aviation, Inc, Canoga Park, California, 7 April 1966.

2. R-6303, Investigation of Catalytic Ignition of Oxygen/Hydrogen Systems, by R. W. Roberts, H. L. Burge, and M. Ladacki, Rocketdyne, a Division of North American Aviation, Inc., Canoga Park, California, December 1965.

3. R-6342-1, Evaluation and Demonstration of the Use of Cryogenic Propellants (O_2-H_2) for Reaction Control Systems, First Quarterly Report, Rocketdyne, a Division of North American Aviation, Inc., Canoga Park California, October 1965.

4. UM 361-66-78, Evaluation and Demonstration of the Use of Cryogenic Propellants (O_2-H_2) for Reaction Control Systems, Tenth Monthly Progress Report, Rocketdyne, a Division of North American Aviation, Inc., Canoga Park, California, 4 May 1966.

5. RR 65-2, Hydrogen Oxygen Catalytic Ignition Studies for Application in the J-2 Engine, by R. Roberts, Rocketdyne, a Division of North American Aviation, Inc., Canoga Park, California, January 1964.

6. UM 361-66-88, Evaluation and Demonstration of the Use of Cryogenic Propellants (O_2-H_2) for Reaction Control Systems, Seventh Monthly Progress Report, Rocketdyne, a Division of North American Aviation, Inc., Canoga Park, California, May 1966.

7. Hunter, B. J., J. E. Bell, and J. E. Penner, "Expulsion Bladders for Cryogenic Fluids," Adv. in Cryogenic Engr., 7 (1961).

8. Pope, D. H., "Expulsion Bladders for Cryogenic Liquids", Adv. in Cryogenic Engr., 10, (1964).

9. Harnett, R. T., F. J. Sanson, and L. M. Warshawsky, "Midas-an-Analog Approach to Digital Computation," Simulation, (September 1964).

10. Belchman, G. E., <u>An Enlarged Version of Midas, Simulation</u>, (October, 1964).

11. Bell Aerosystems Company, "Feasibility Demonstration of Advanced Attitude Control Systems," AFRPL-TR-62-251 (November 1965), CONFIDENTIAL.

12. Bell Aerosystems Company, "Feasibility Demonstration of Advanced Attitude Control Systems," AFRPL-TR-66-55 (March 1966) CONFIDENTIAL.

TABLE 1

THRUSTOR COMPUTER PROGRAM PLAN

Task No.

I.   Investigation of thrustor pneumatic and thermal responses for:
      1. Full flow
      2. Downstream injection

II.   Investigation of startup and shutdown transients
      1. Define transient mixture ratio variations
      2. Investigate remedies by:
         a. Valve sequencing
         b. Fixing the ratio of preinjector volumes

III. Pulse-mode analysis
      1. Experimental thrustor
      2. Best engine geometry

IV.   Investigation of the effect of accumulator parameters on
      thrustor performance
      1. Variation of inlet pressure from nominal
      2. Temperature deadband
      3. Injector face and catalyst bed pressure drop
      4. Nominal inlet pressures
      5. Full flow vs DSI

TABLE 2

OVERALL MATERIAL BALANCE FOR STEADY-STATE

OPERATION OF PROPOSED CONDITIONER

Case No.	Propellant at Conditioner Inlet or Propellant Tanks				Propellant at Gas Generators			Percent of Total Flow to Gas Generator	Propellant at Thrustor	
	Oxygen State	$\dot{w}_o$, lb/sec	Hydrogen State	$\dot{w}_f$, lb/sec	MR, o/f	$\dot{w}_o$, lb/sec	$\dot{w}_f$, lb/sec		$\dot{w}_o$, lb/sec	$\dot{w}_f$, lb/sec
I	O_2 Liquid	0.03852	Liquid H_2 with 5-percent He	0.01642	1.32	0.002822	0.002121	9.0	0.0357	0.0143
II	O_2 Liquid	0.0388	H_2 Liquid	0.0174	1.00	0.00309	0.00309	11.0	0.0357	0.0143
III	O_2 Vapor	0.03722	H_2 Vapor	0.01582	1.0	0.00152	0.00152	5.73	0.0357	0.0143

TABLE 3

DETAILS FOR STEADY-STATE OPERATION OF PROPOSED
DESIGN OF OXYGEN HEAT EXCHANGER

Hot Side

Case No.	Propellant Flowrate $\dot{w}_o$, lb/sec	$\dot{w}_f$, lb/sec	MR	T_c, R	T_{outlet}, R	ID, inches	ΔP, psi	h_g, $\frac{Btu}{hr\text{-}ft^2\text{-}F}$	Area, sq in.	L, inches
I	0.000778	0.000585	1.33	2500	672	0.335	8.0	59.2	--	105.0
II	0.00080	0.00080	1.00	2000	672	0.354	8.0	59.2	136.0	122.2
III	0.0000596	0.0000596	1.00	2000	672	--	--	--	--	--

Cold Side

Case No.	$\dot{w}_o$, lb/sec	T_i, R	T_o, R	q, $\frac{Btu}{seconds}$	ΔP, psi	h_ℓ, $\frac{Btu}{hr\text{-}ft^2\text{-}F}$	h_g, $\frac{Btu}{hr\text{-}ft^2\text{-}F}$	U_ℓ	U_g
I	0.03852	163	200	3.85	1.0	18.1	72.7	13.1	32.6
II	0.03879	163	200	3.86	1.0	18.1	72.7	13.9	32.6
III	0.03722	163	200	0.2905	--	--	--	--	--

$\dot{w}_o$ = oxidizer weight flowrate
$\dot{w}_f$ = fuel weight flowrate
MR = mixture ratio, o/f
T_c = combustion temperature
T_{outlet} = temperature at heat exchanger outlet
ID = inside diameter
ΔP = differential pressure
h_g = heat transfer coefficient (gas)

h_ℓ = heat transfer coefficient (liquid)
L = length
T_i = inlet oxidizer temperature
T_o = heat exchanger outlet oxidizer temperature
q = heat exchanger heat load
U_ℓ = overall heat transfer coefficient (liquid)
U_g = overall heat transfer coefficient (gas)

TABLE 4

PROPOSED STEADY-STATE DESIGN OF HYDROGEN HEAT EXCHANGER

Hot Side

Case No.	Propellant Flowrate		MR	T_c, R	T_{outlet}, R	ID, inch	ΔP, psi	h_g, Btu/hr-ft²-F	Area sq in.	L, inches
	$\dot{w}_o$, lb/sec	$\dot{w}_f$, lb/sec								
I	0.0020044	0.001536	1.33	2500	672	0.46	8.0	71.4	--	70.0
II	0.00229	0.00229	1.0	2000	672	0.50	8.0	71.4	--	86.6
III	0.00146	0.00146	1.0	2000	672	--	--	--	--	--

Cold Side

Case No.	$\dot{w}_o$, lb/sec	T_i, R	T_o, R	q, Btu/seconds	ΔP, psi	h_ℓ, Btu/hr-ft²-F	h_g, Btu/hr-ft²-F	U_ℓ	U_g
I	0.01642	37	200	10.13	1.0	39.2	275	25.4	56.7
II	0.01739	37	200	11.20	1.0	39.2	275	25.4	56.7
III	0.01582	37	200	7.12	--	--	--	--	--

$\dot{w}_o$ = oxidizer weight flowrate

$\dot{w}_f$ = fuel weight flowrate

MR = mixture ratio

T_c = combustion temperature

T_{outlet} = temperature at heat exchanger outlet

ID = inside diameter

ΔP = differential pressure

h_g = heat transfer coefficient (gas)

h_ℓ = heat transfer coefficient (liquid)

L = length

T_i = inlet oxidizer temperature

T_o = heat exchanger outlet oxidizer temperature

q = heat exchanger heat load

U_ℓ = overall heat transfer coefficient (liquid)

U_g = overall heat transfer coefficient (gas)

46

TABLE 5

GAS GENERATOR PARAMETERS

Parameter	Hydrogen Gas Generator	Oxygen Gas Generator
Diameter, inches	1.0	0.625
Weight Flowrate, lb/sec		
Oxygen	0.00229	0.0008
Hydrogen	0.00229	0.0008
Superficial Mass Velocity, lb/sec-sq in.	0.00584	0.00521
Velocity, ft/sec (Mixer)	36.8	33.0
Pressure Drop, psi		
Valve	0.5	0.5
Injector Face	2.5	2.5
Mixer Section	0.5*	0.5*
Catalyst Bed	3.5	3.5
Areas, sq in.**		
Injector Face		
Hydrogen	0.02494	0.00871
Oxygen	0.00626	0.00219
Throat (Mixture Ratio = 1.0)	0.10335	0.03611

*1/2 inch of 1/8-inch beads

**C_D A where C_D = 0.73

TABLE 6

HEAT EXCHANGER DATA

For Case I in Tables 2, 3, and 4

Parameter	Hydrogen Heat Exchanger	Oxygen Heat Exchanger
Cold Side Length, inches		
Liquid Phase	34	101.5
Gas Phase	36	3.5
Heat Transfer Coefficient, $Btu/hr-ft^2-F$		
Cold Side		
Liquid Phase	39.2	18.1
Gas Phase	275	72.7
Hot Side	71.4	59.2

Left section

Col	NUMBER	DESCRIPTION
1	1	
13	0. 0 0 2	CALC. TIME INCRE.
25	5 0 . 0	PRINT EVERY 50TH PT.
37	2 . 0	RUN DURATION
49	1 9 9 9	GG DEAD BAND
61	5 . 0	ACC. TEMP. D.B.
IDENTIFICATION 73		1.0 80

Col	NUMBER	DESCRIPTION
1	6	
13	0. 5 . 0	ACC. PRESS. D.B.
25	1 2 0 . 0	WALL TEMP. D.B.
37	2 0 0 . 0	NOT USED
49	0 . 0	ACC. HEAT LEAK
61	0 . 0	HEATER ELEC.
IDENTIFICATION 73		2.0 80

Col	NUMBER	DESCRIPTION
1	11	
13	0. 0 2	MAIN PROP. DELAY
25	0. 0 7	GG VALVE DELAY
37	0.	A RAT $\emptyset$
49	1 0 . 0	LINE VOL.
61	4 . 0	GG INJ. VOL.
IDENTIFICATION 73		3.0 80

Col	NUMBER	DESCRIPTION
1	16	
13	8 . 0	GG CHAMBER VOL.
25	1 1 . 5	HOT SIDE VOL.
37	2 5 0 . 0	ACC. VOL.
49	0 . 0	AMPL. OF GG
61	1 . 0	FREQ.
IDENTIFICATION 73		4.0 80

Right section

Col	NUMBER	DESCRIPTION
1	2 1	
13	0. 6 0	THR. FLOW DELAY
25	0. 0 3 6	THR. O_2 FLOW
37	1 . 0	THR. FREQ.
49	1 . 0	THR. DUTY CYCLE
61	0 . 0	AMP LH_2 TANK PRES.
IDENTIFICATION 73		5.0 80

Col	NUMBER	DESCRIPTION
1	2.6	
13	1 . 0	FREQ. H_2 TANK PRES.
25	2 0 . 0	TW INIT.
37	2 0 0 . 0	GG TEMP.
49	2 0 0 . 0	CAT TEMP.
61	2 0 0 . 0	ACC. TEMP.
IDENTIFICATION 73		6.0 80

Col	NUMBER	DESCRIPTION
1	3 1	
13	4 0 . 0	WALL TEMP.
25	2 0 . 0	NOT USED
37	2 2 . 6	THERMAL RES. O_2 L
49	2 4 1	THERMAL RES. O_2 g
61	1 8 0	THERMAL RES. HOT SIDE
IDENTIFICATION 73		7.0 80

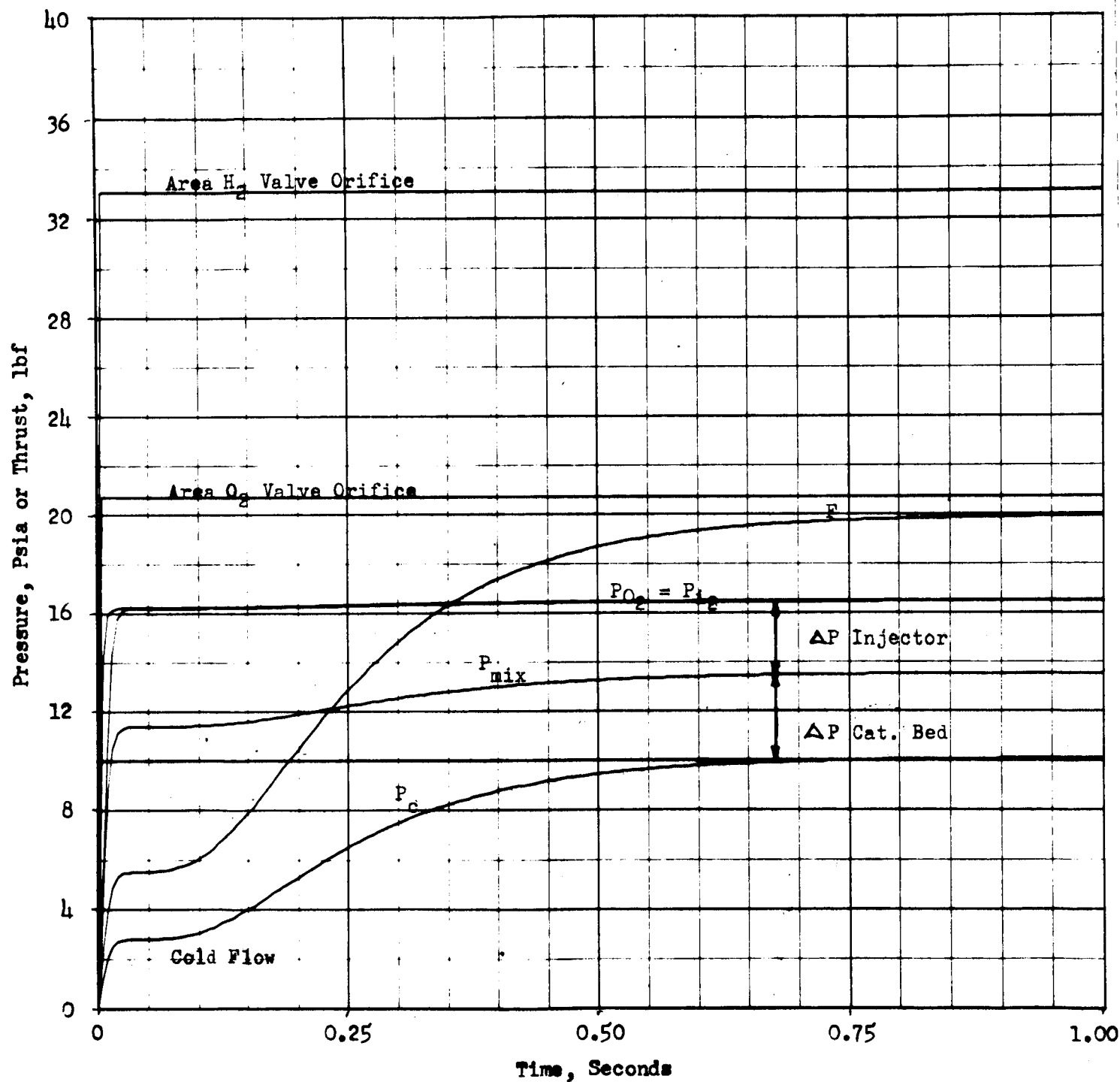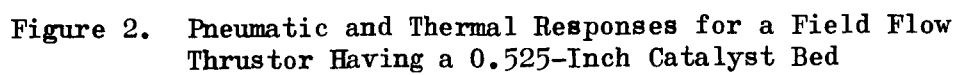| Col	NUMBER	DESCRIPTION
1	3.6	
13	0. 0 9 7	WALL HEAT CAPACITY
25	1 . 0	PLT FLOWS
37	0 . 0	GAS FEED - 0.
49		LIQUID FEED - l.
61		
IDENTIFICATION 73		8 0 80

FORM 609-W-23 NEW 1-65

49

Figure 1. Pneumatic and Thermal Responses for a Full Flow
Thrustor Having a 0.525" Catalyst Bed

Figure 2. Pneumatic and Thermal Responses for a Field Flow
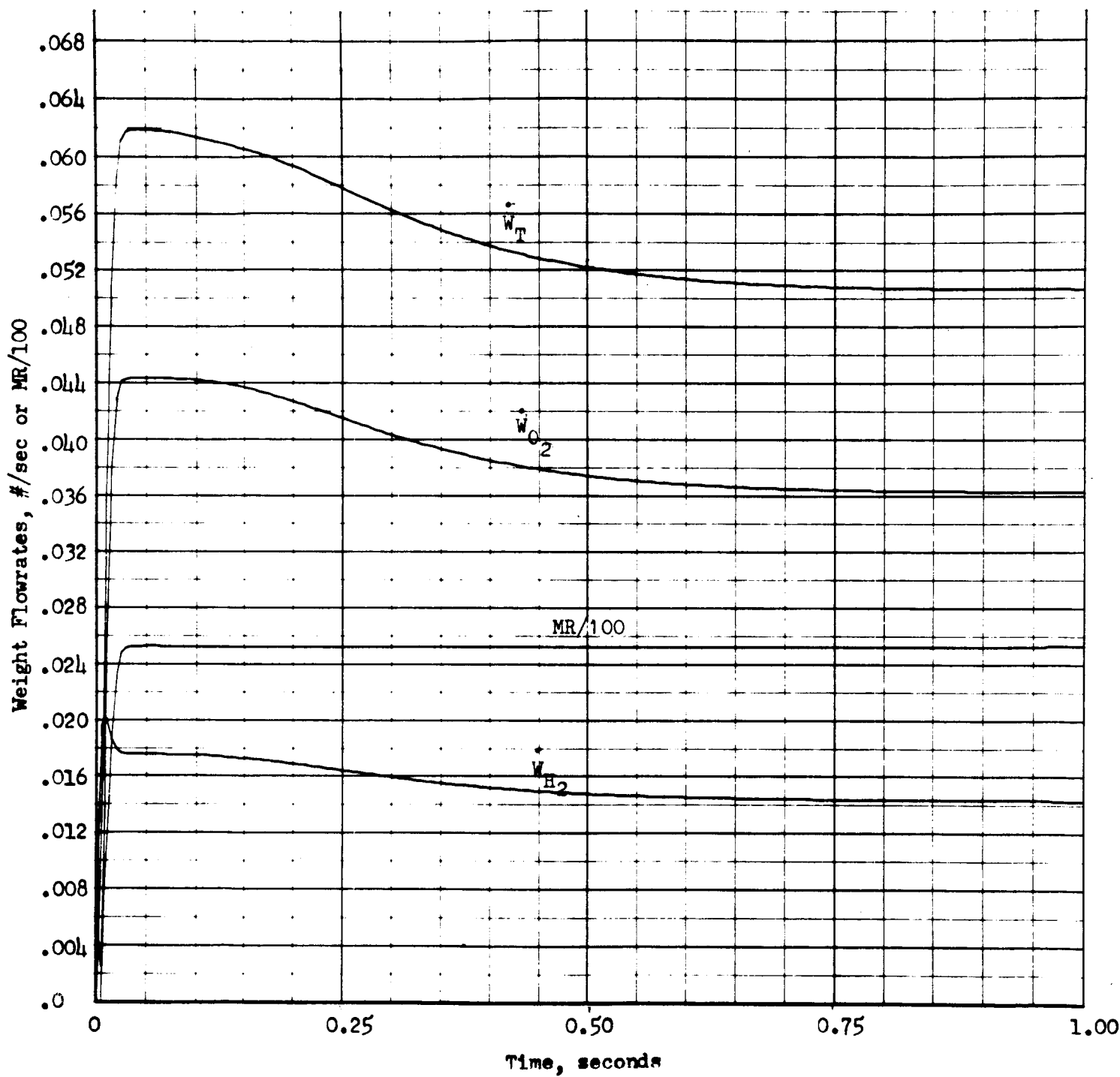Thrustor Having a 0.525-Inch Catalyst Bed

Figure 3. Pneumatic and Thermal Responses for a Full Flow
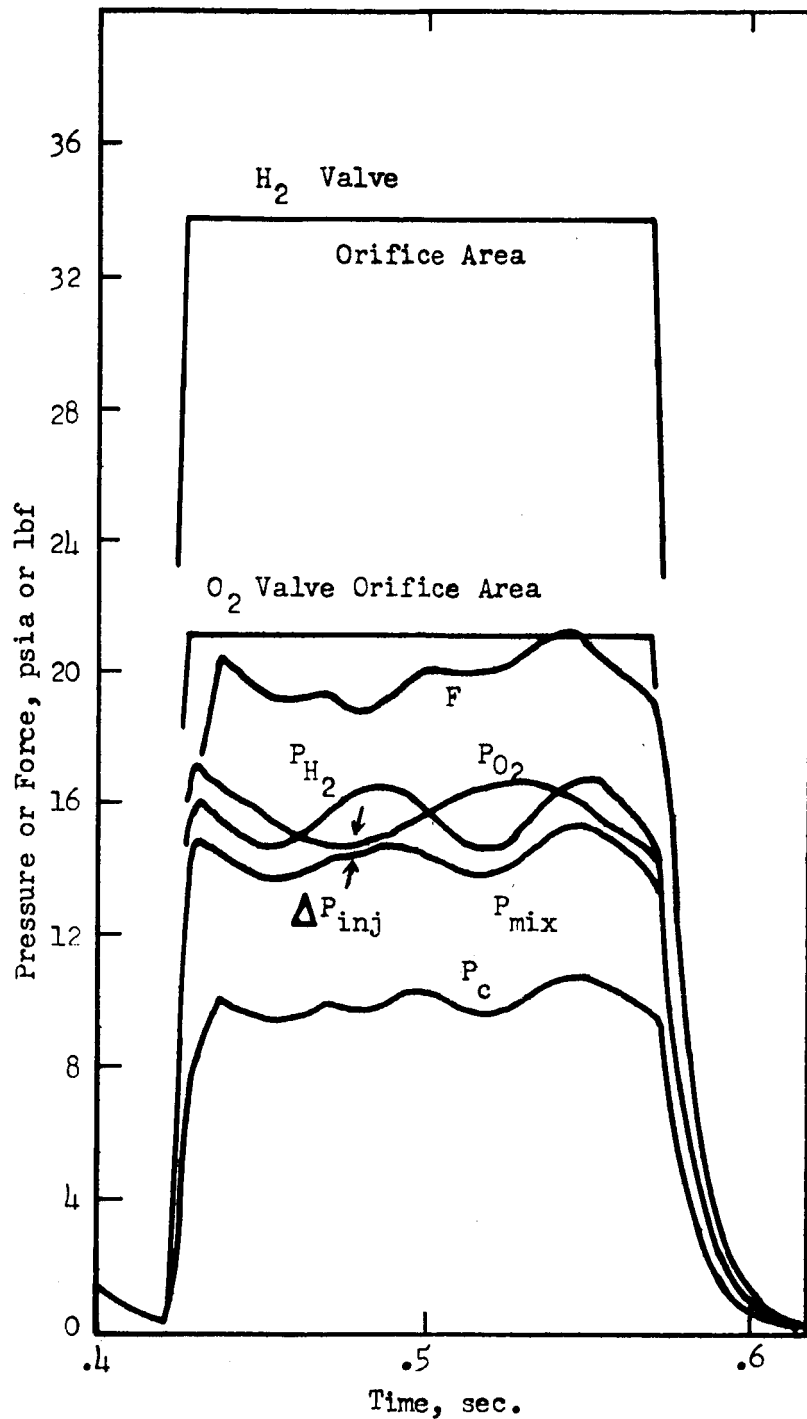Thrustor Having a 0.525-Inch Catalyst Bed

Figure   4.   Thrustor Chug Analysis for Worst Oxydizer Rich
Case with the Following Input Data

  a. $17.5 = P_{O_2}$ or $P_{H_2} = 16.25 + 1.25 \sin wt$

  . $W_{O_2} = 10$ cps $W_{H_2} = 15$ cps

  b. $T_{O_2} = 180R$, $T_{H_2} = 220R$

  c.   1 inch bed length with a linear temperature
      rise across first 2 inches of bed
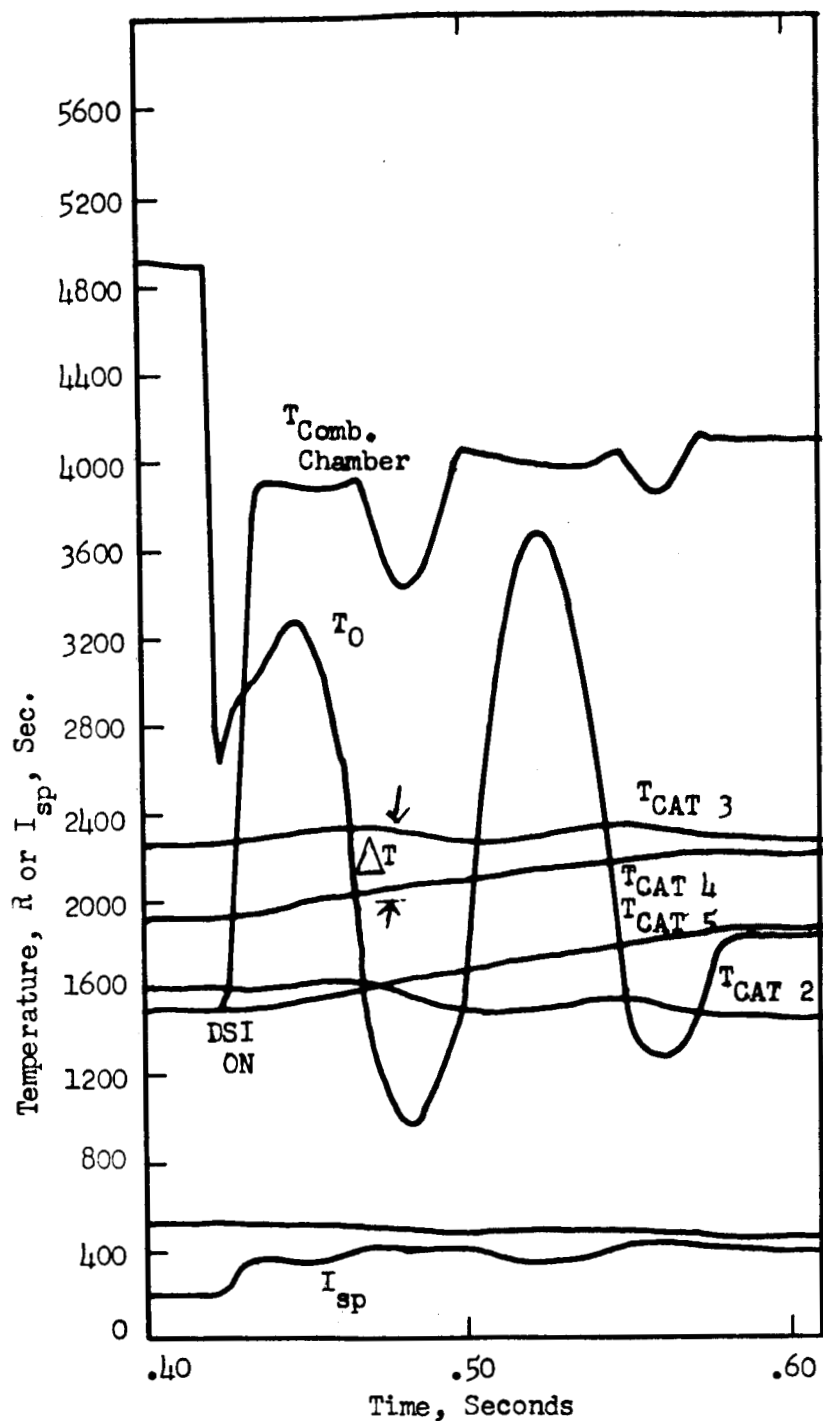
Figure   5.   Thermal Responses of a 1" Length Catalyst
Bed Divided into Five 0.2" Nodes with the
Nominal Steady State Temperatures being:

$T_{CAT\ 1} = 400°R$, $T_{CAT\ 2} = 1200°R$, $T_{CAT\ 3} = 1200$,
$T_{CAT\ 4} = T_{CAT}5 = 2000°R$

Note changes in catalyst bed node temperatures from nominal
caused by being oxidizer rich.

54
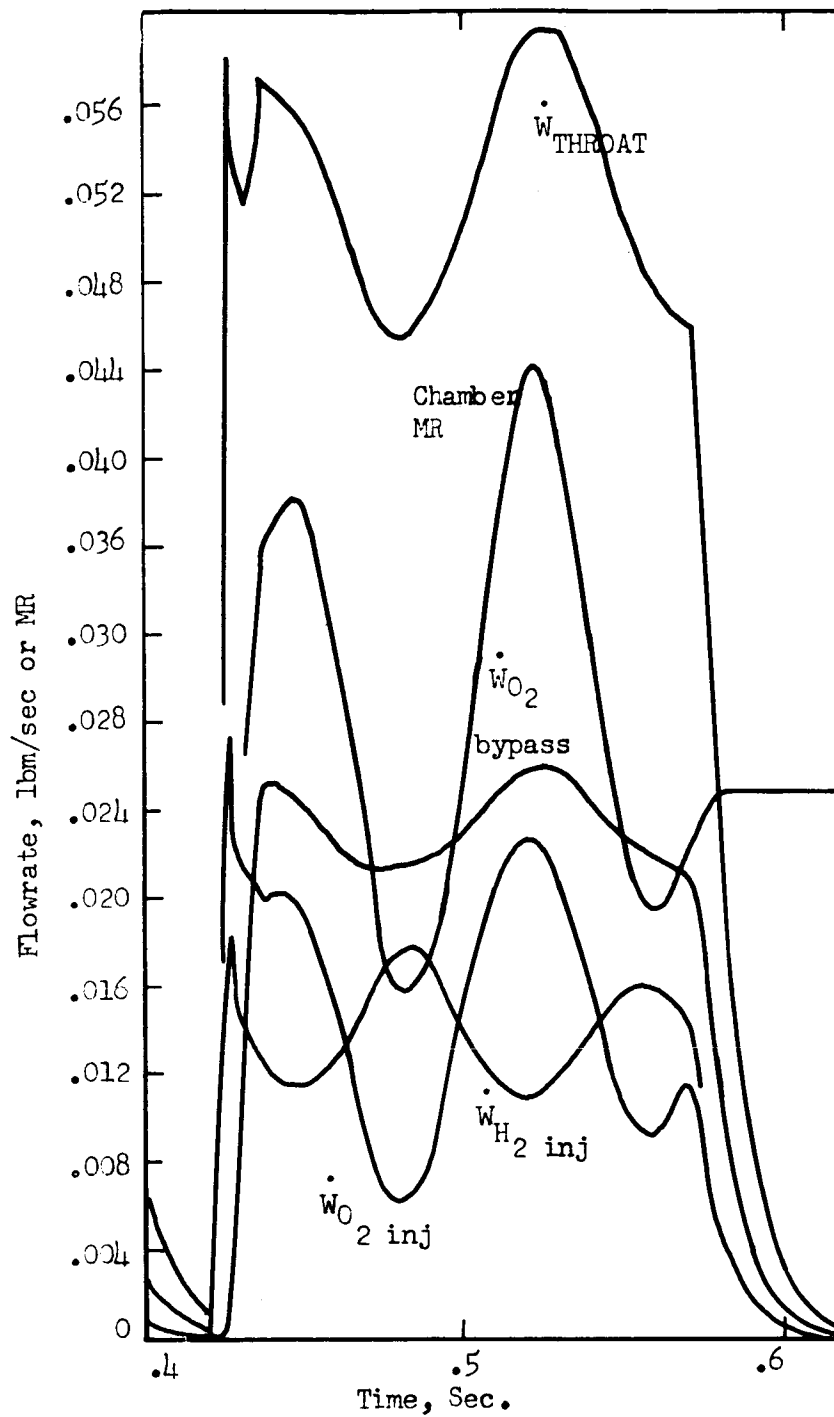
Figure   6.   Injector and Throat Flow Rates and Chamber
               Mixture Ratio.

Note how throat flowrate follows O_2 flowrate at nominal design
there is 2.5 lbm of O_2 flowing per lbm of H_2.
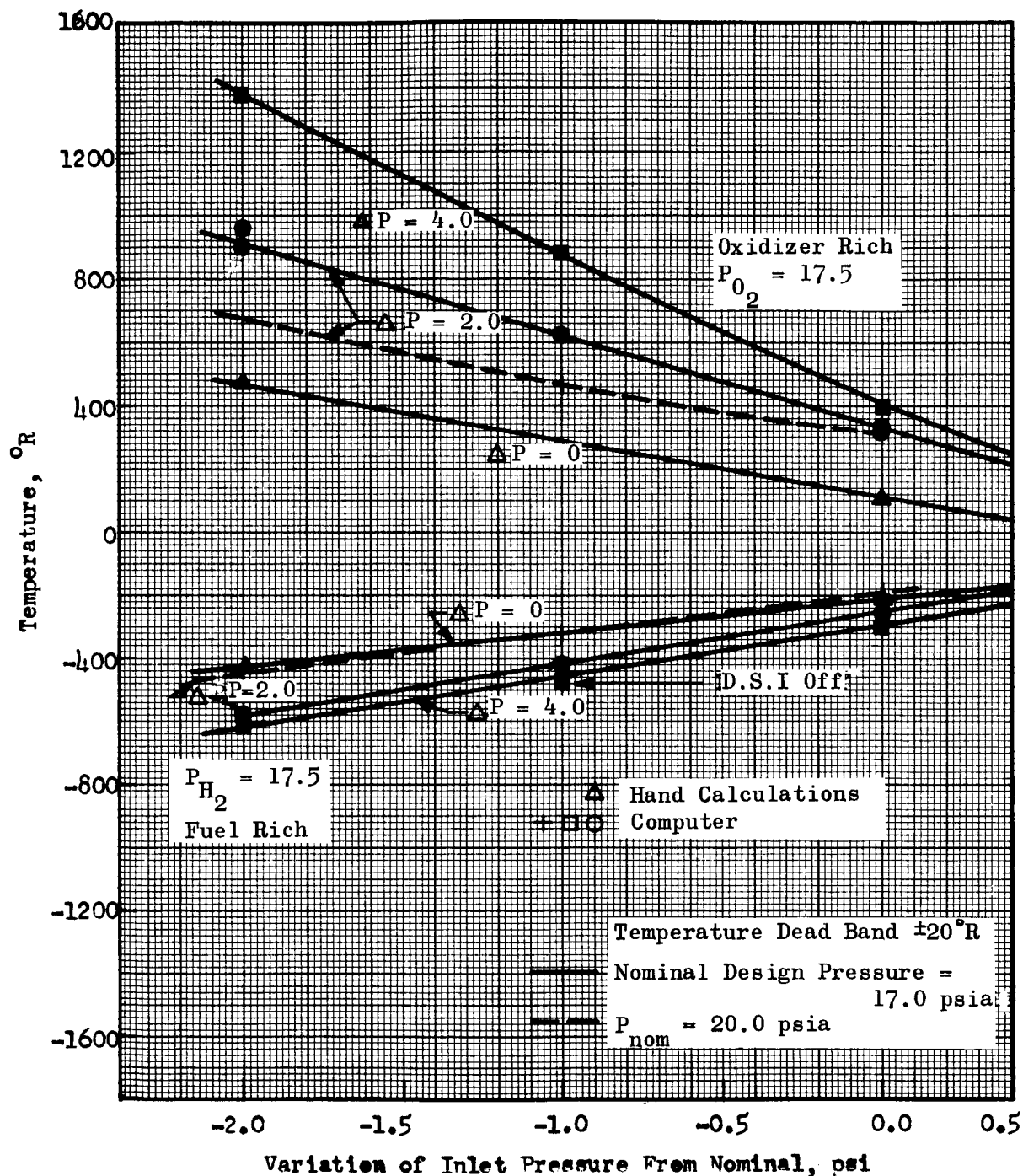
Figure 7. Change in Catalyst Bed Combustion Temperature as a Function of Inlet Pressure for D.S.I. With Catalyst Bed Pressure Drop and Nominal Pressure as Parameters
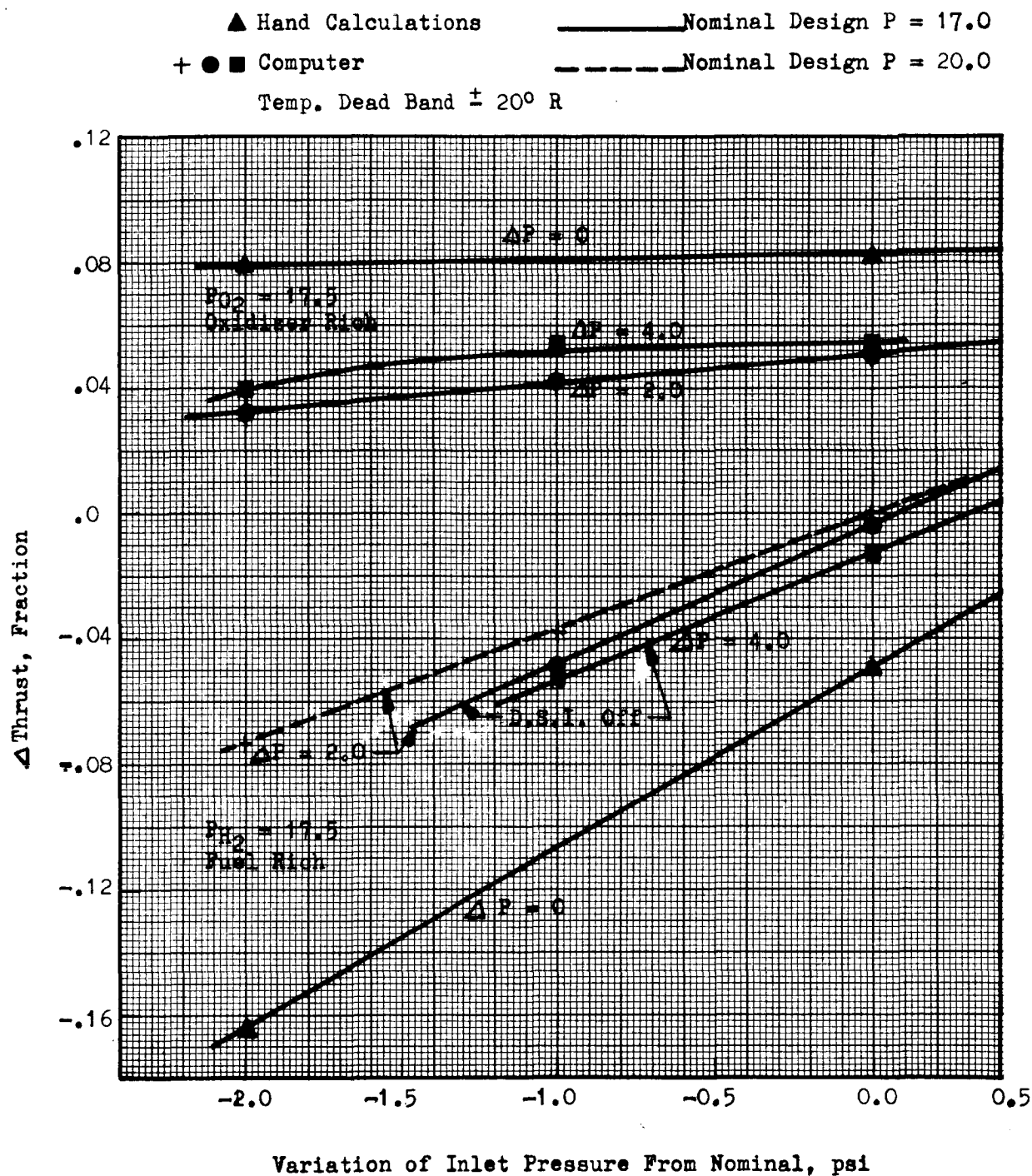
Figure 8. Change in Thrust as a Function of Inlet Pressure for D.S.I. With Nominal Pressure and Bed Pressure Drop as Parameters.
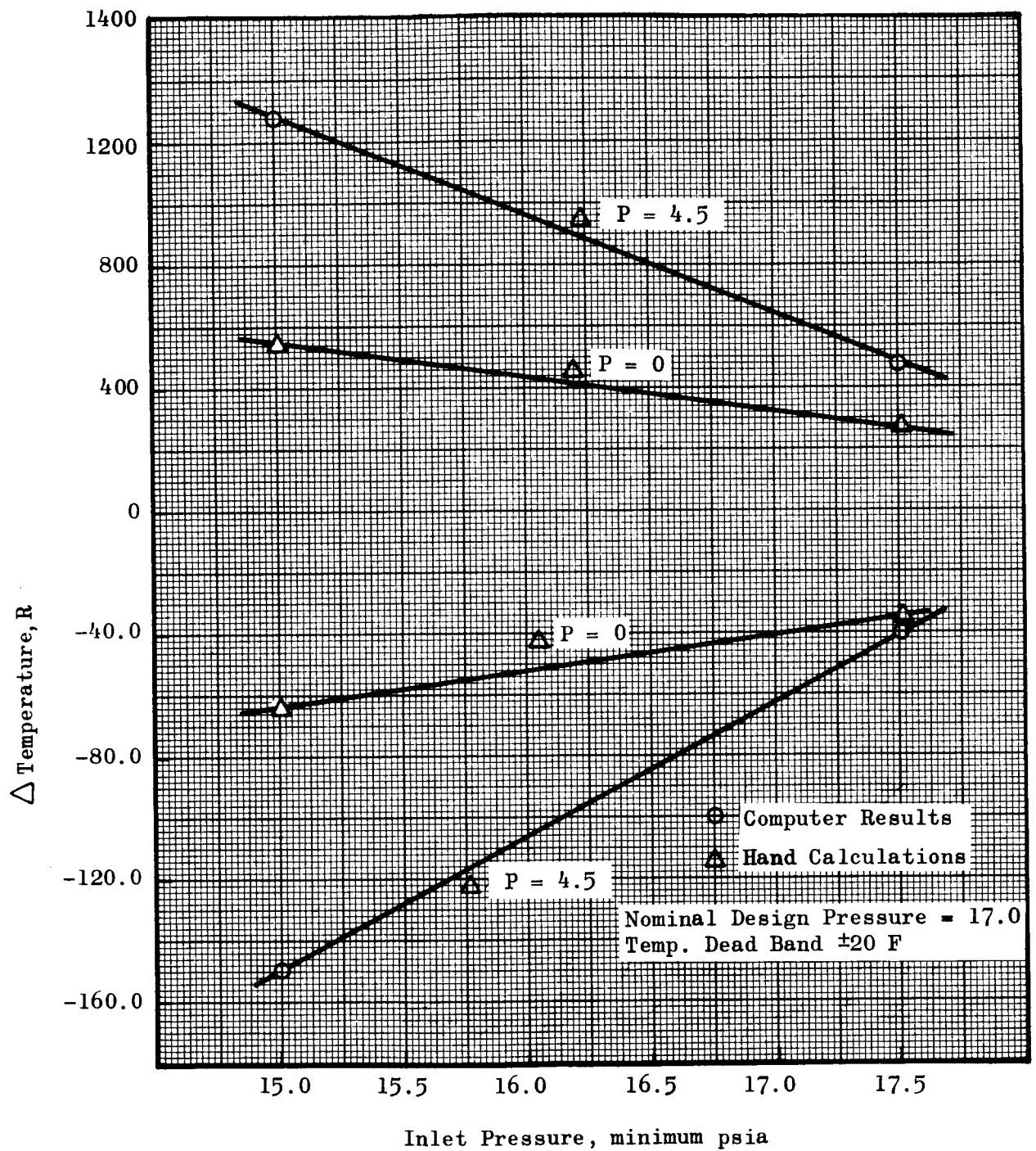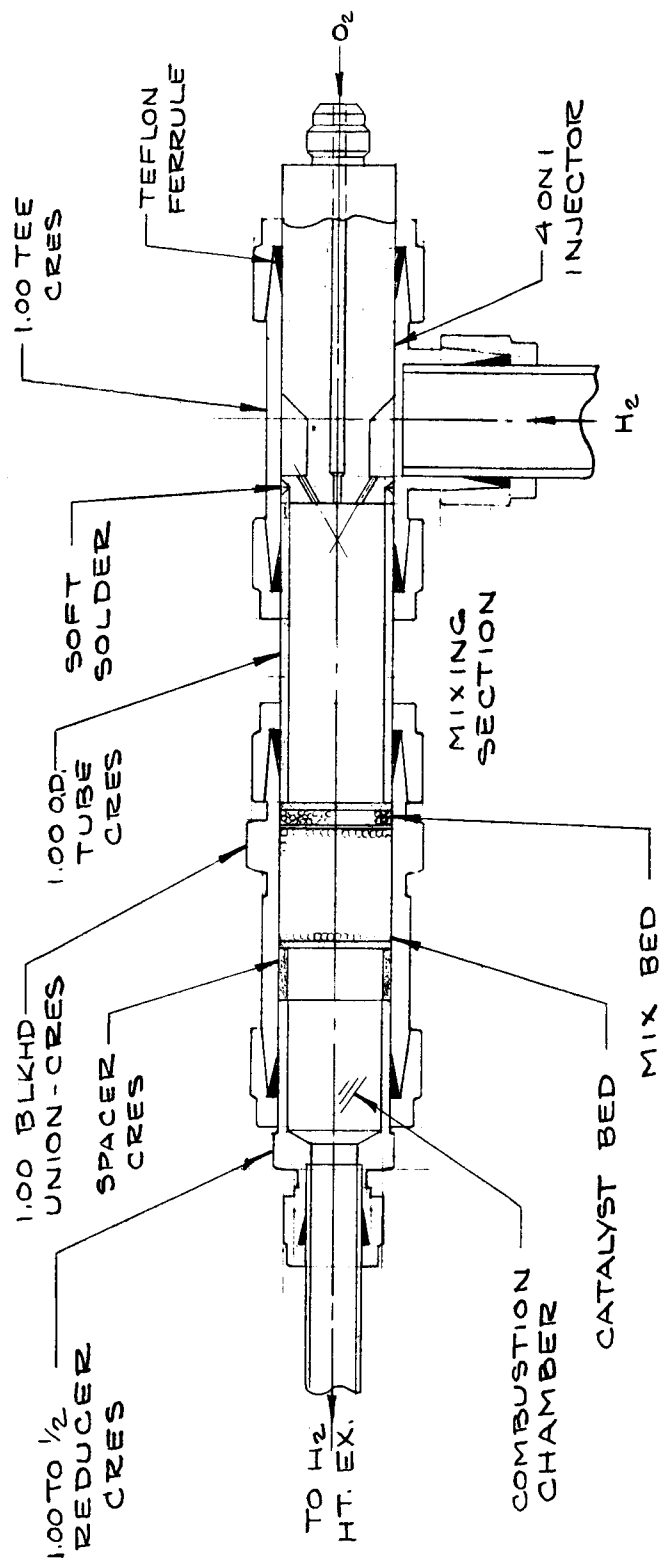
1400

1200

800

400

0

−40.0

−80.0

−120.0

−160.0

△ Temperature, R

P = 4.5

P = 0

P = 0

P = 4.5

⊕ Computer Results
△ Hand Calculations

Nominal Design Pressure = 17.0
Temp. Dead Band ±20 F

15.0   15.5   16.0   16.5   17.0   17.5

Inlet Pressure, minimum psia

Figure 9.   Changes in Catalyst Bed Combustion Temperature as a
Function of Inlet Pressure for Full Flow With Catalyst
Bed Pressure Drop as a Parameter

58

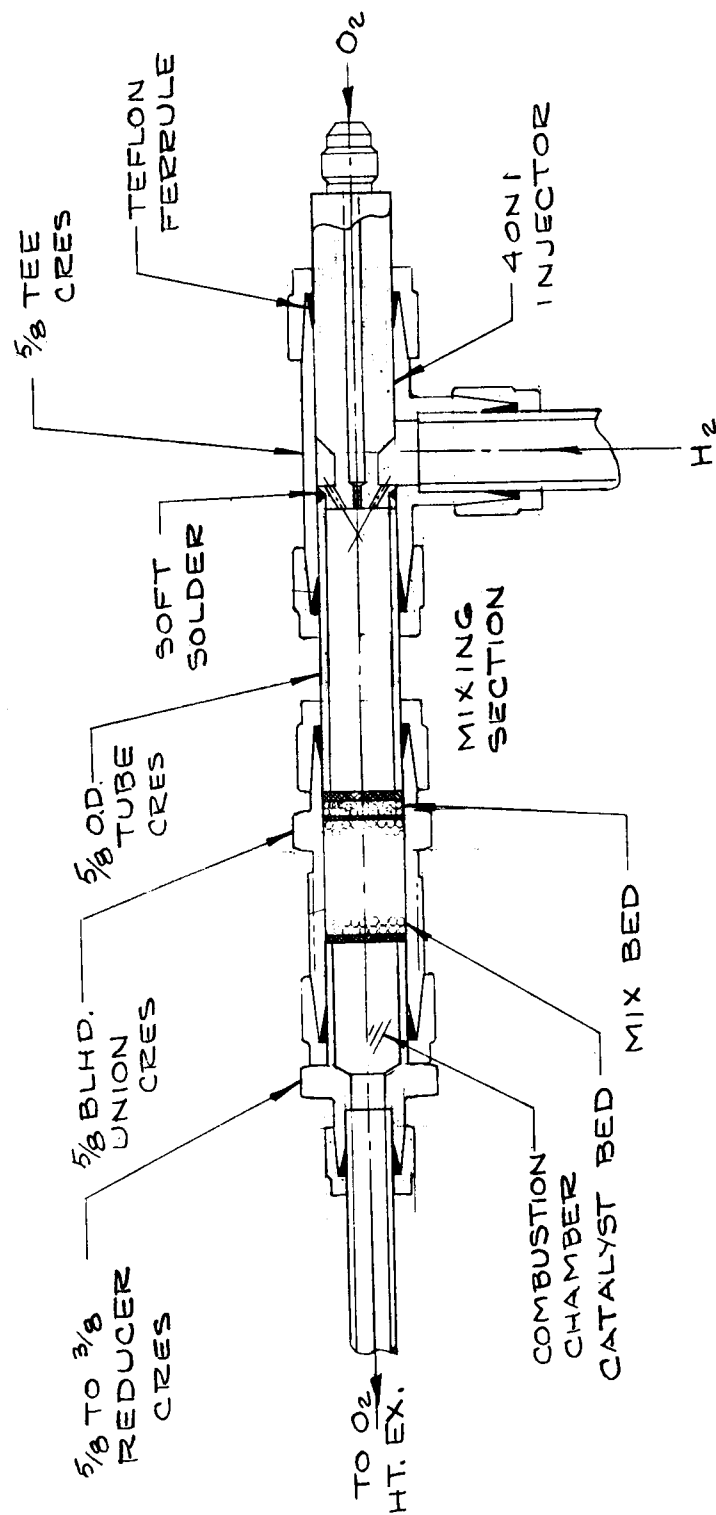Figure 10. Full-Scale Schematic of the H_2 Heat Exchanger Gas Generator

59

Figure 11. Full-Scale Schematic of the O_2 Heat Exchanger Gas Generator
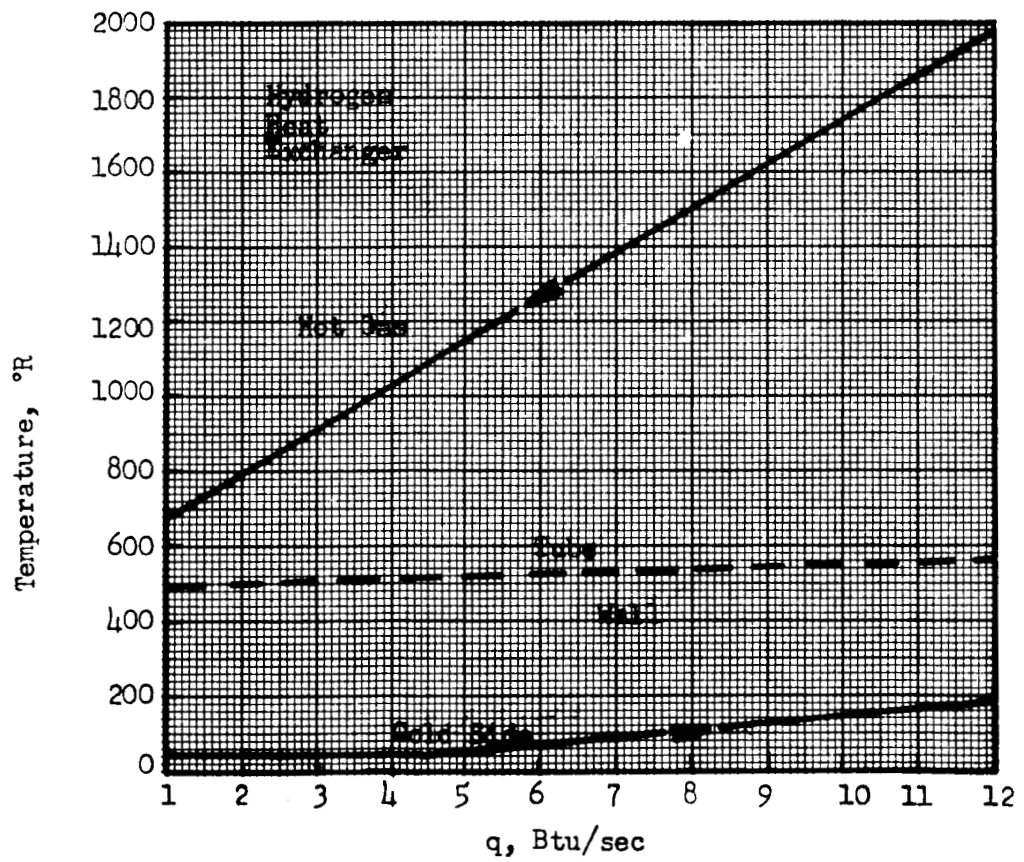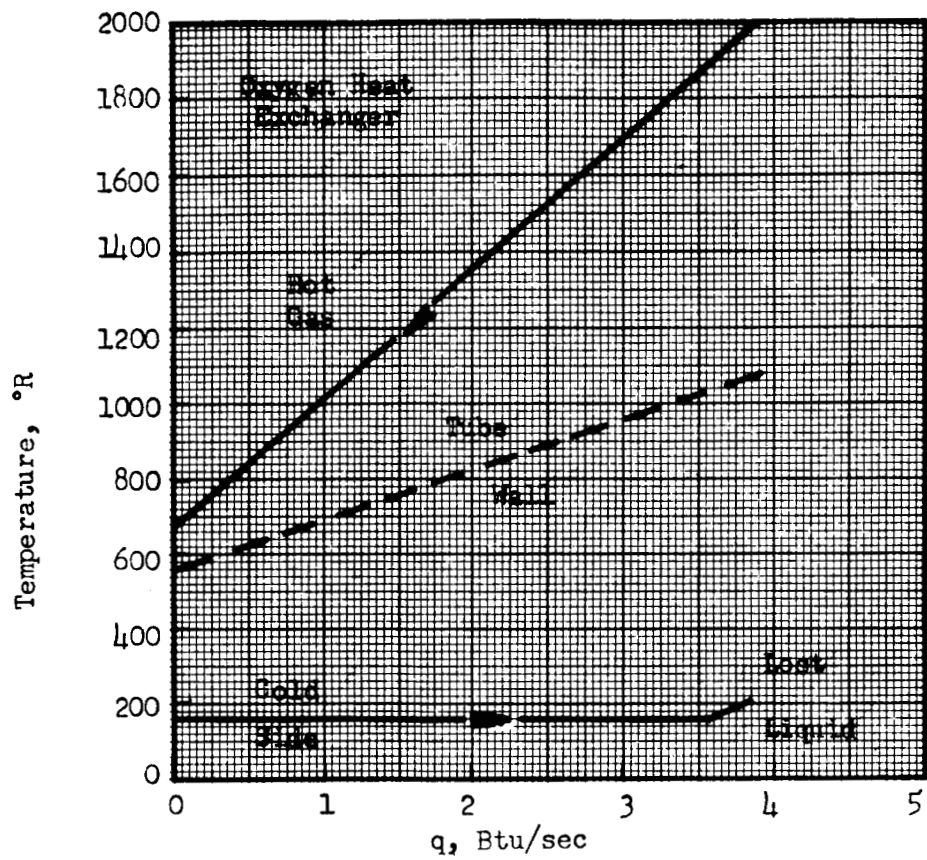
60

Figure 12. Steady State Temperature Profiles for the H_2 and O_2 Heat Exchangers.
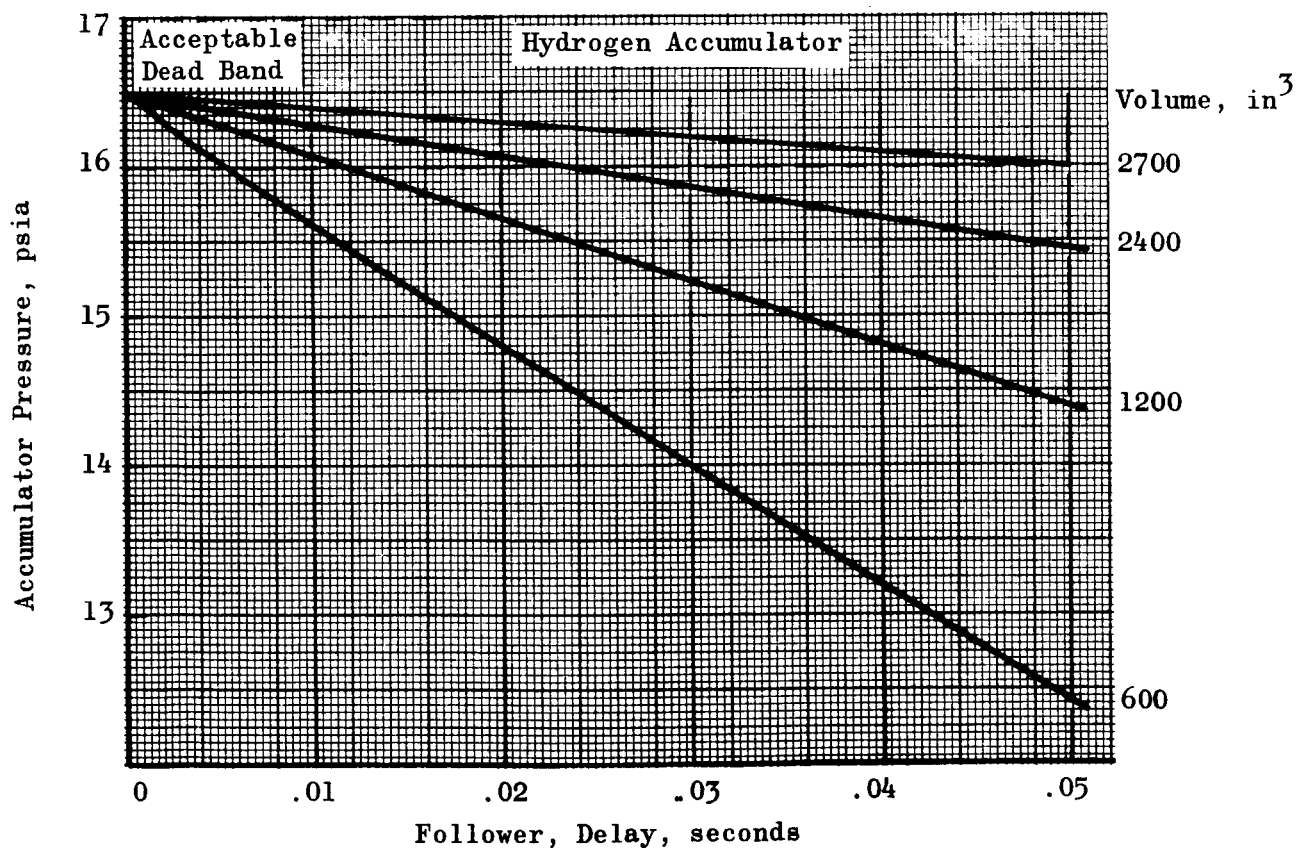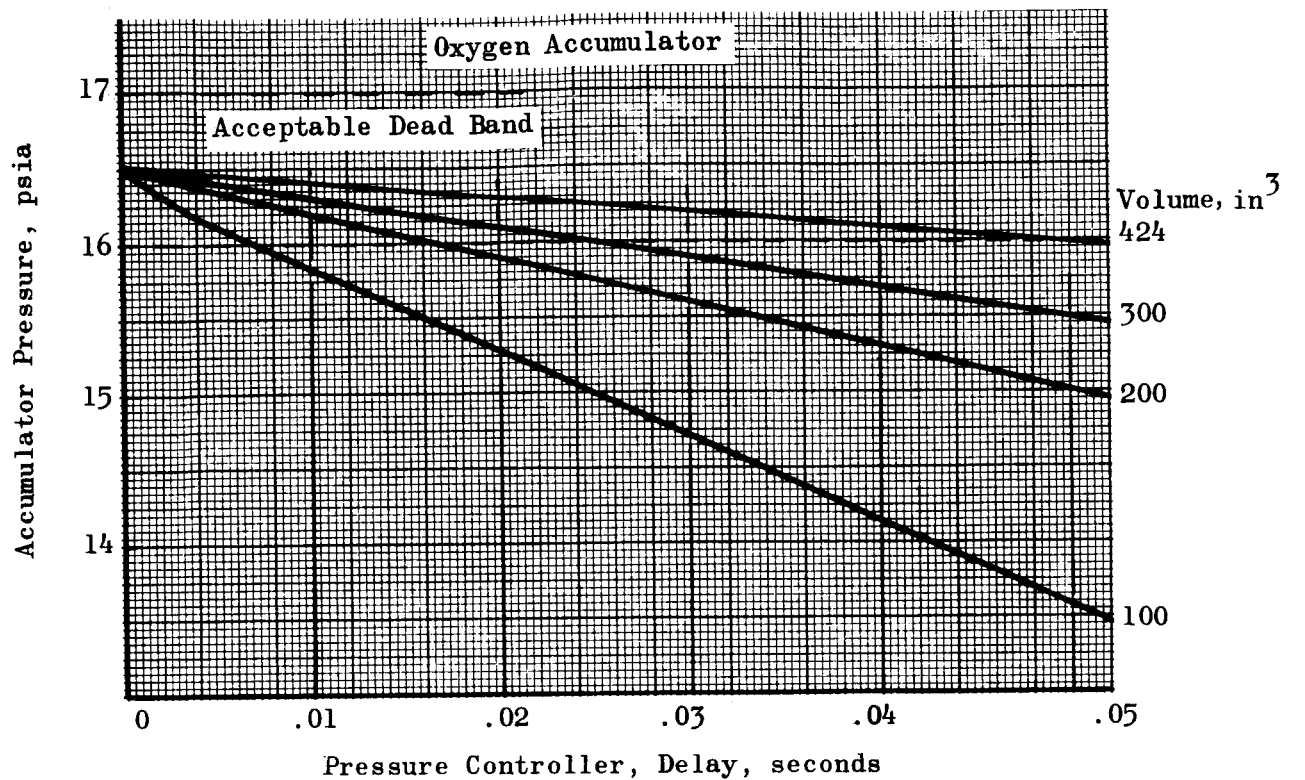
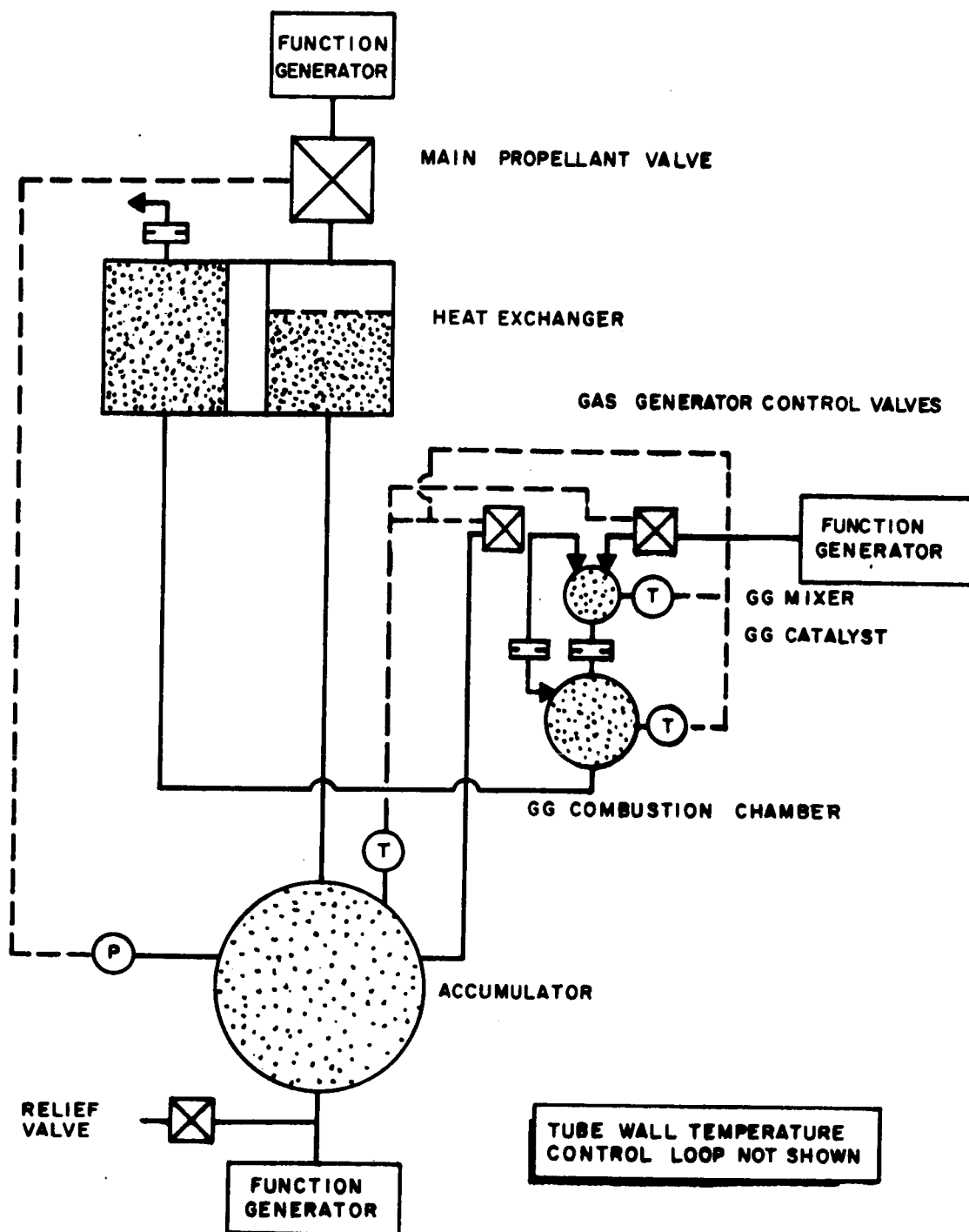Figure 13. Accumulator Sizing Chart Based on Valve Response

Figure 14. Conditioner Model Schematic
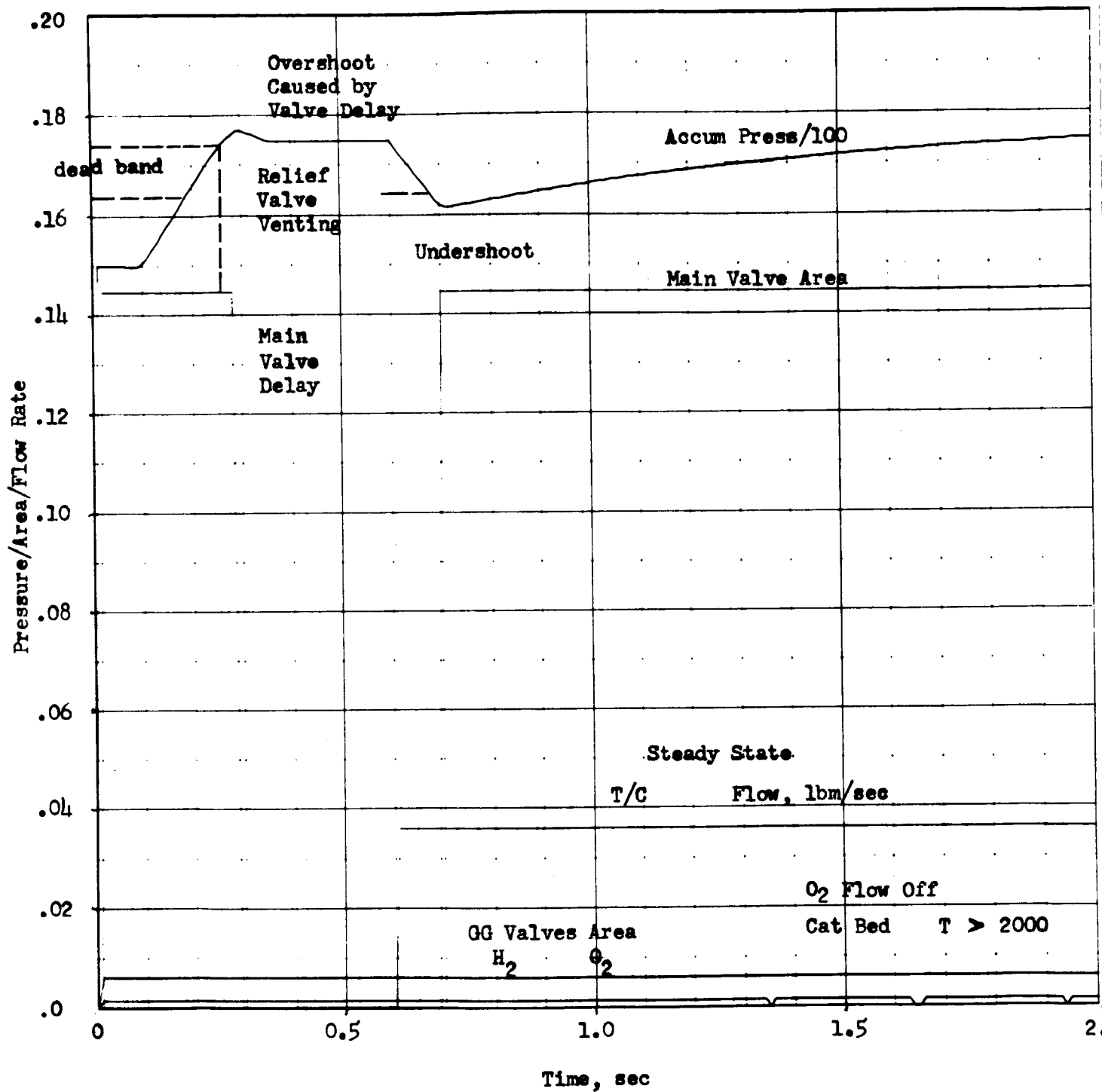
Figure 15. Conditiener System Dynamics for Saturated Vapor from Propellant Tank-O_2 With a Steady State Thrustor Demand
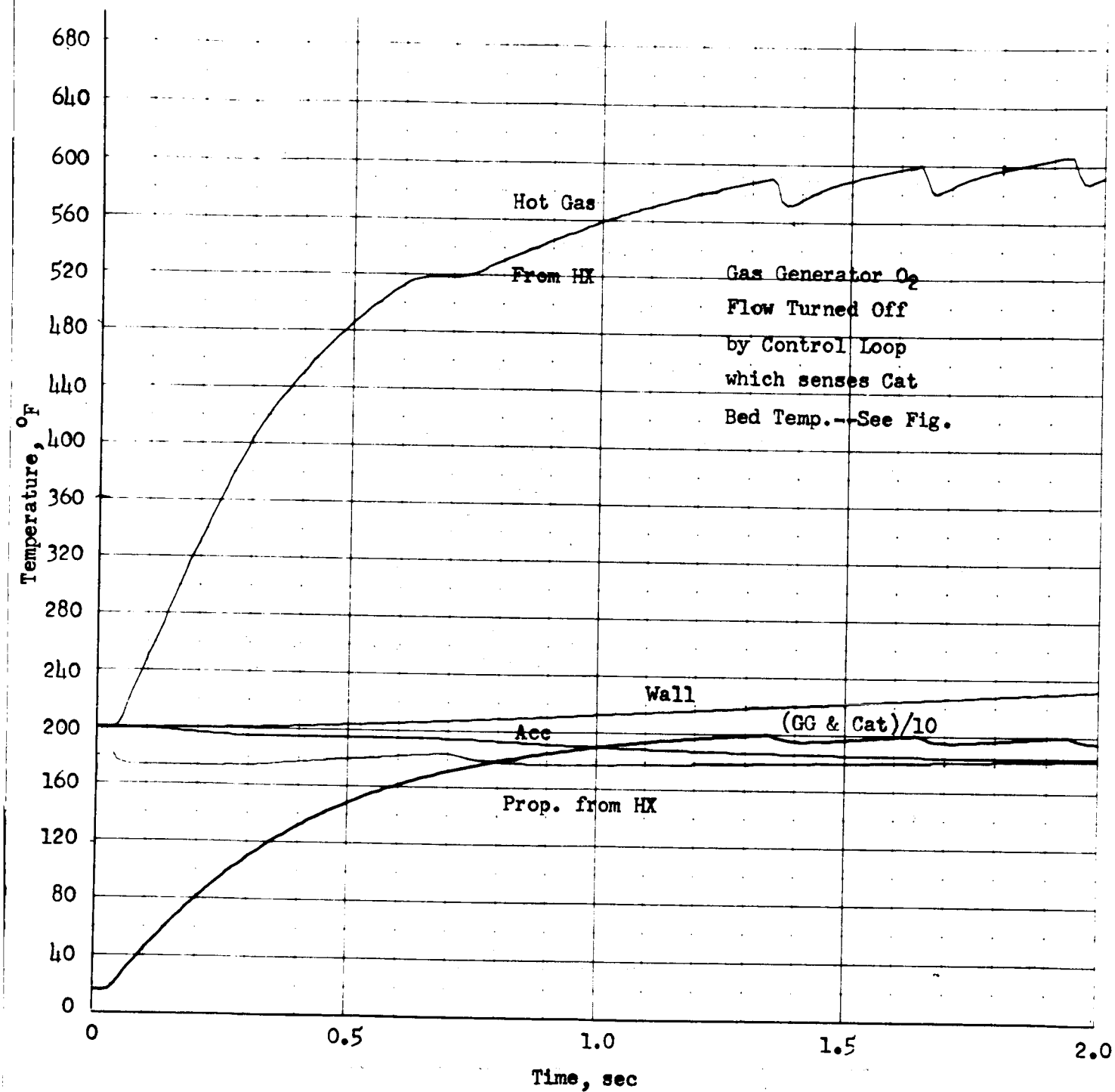
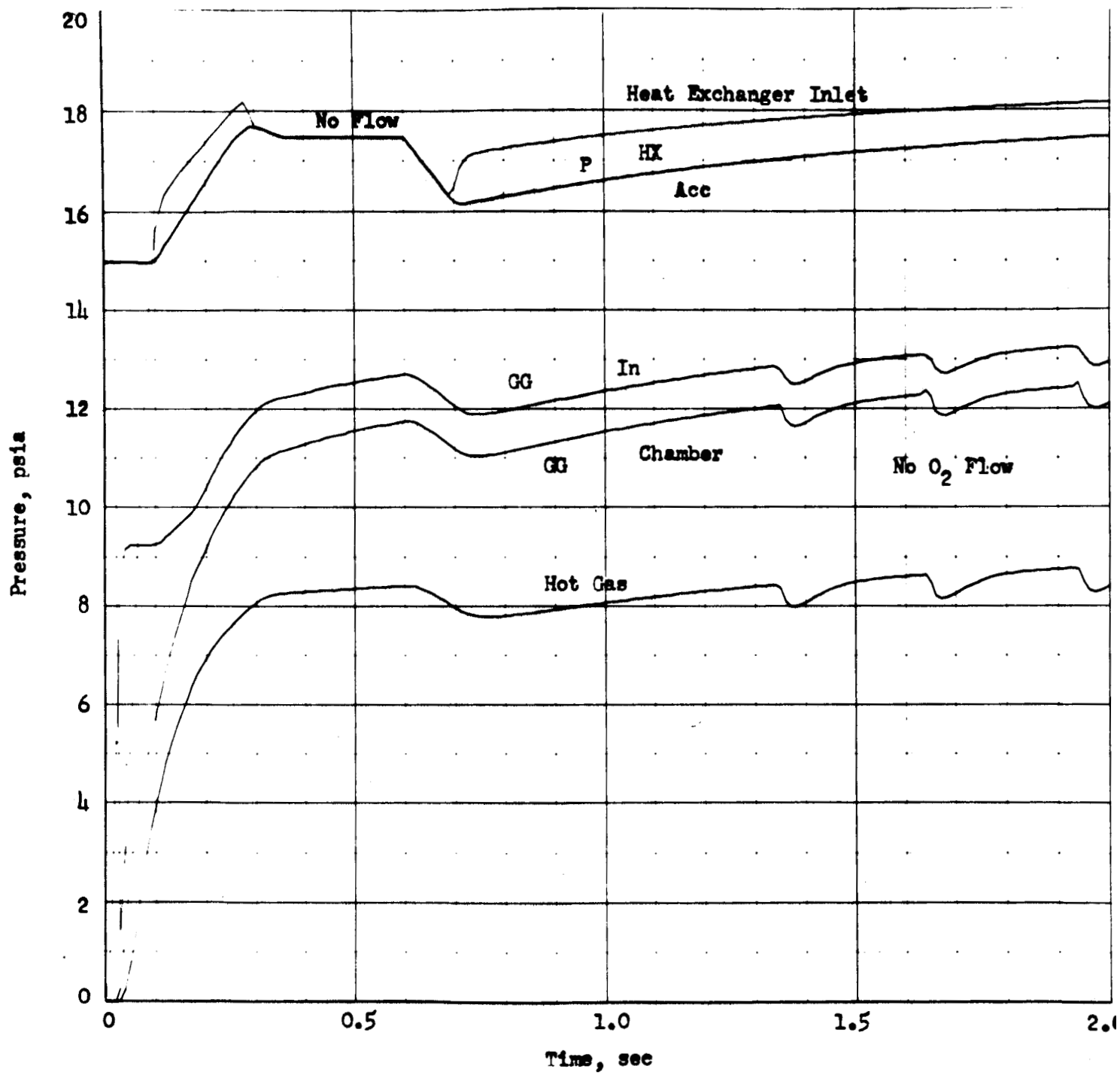Figure 16. Thermal Responses for the O_2 Conditioning System

Figure 17. Pressure Responses for the O_2 Conditioning System
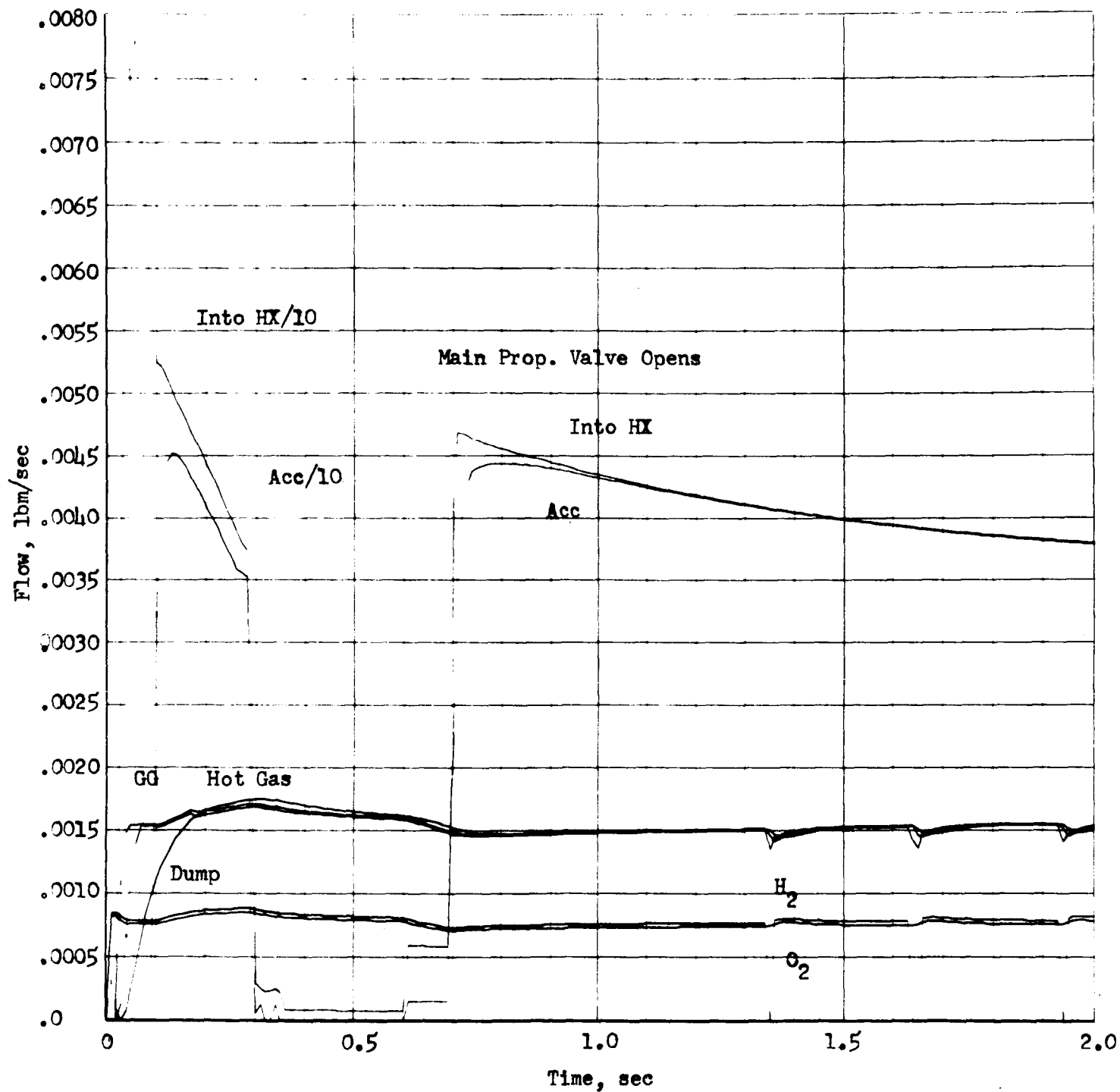
66

Figure 18. Weight Responses for an O_2 Conditioning System With
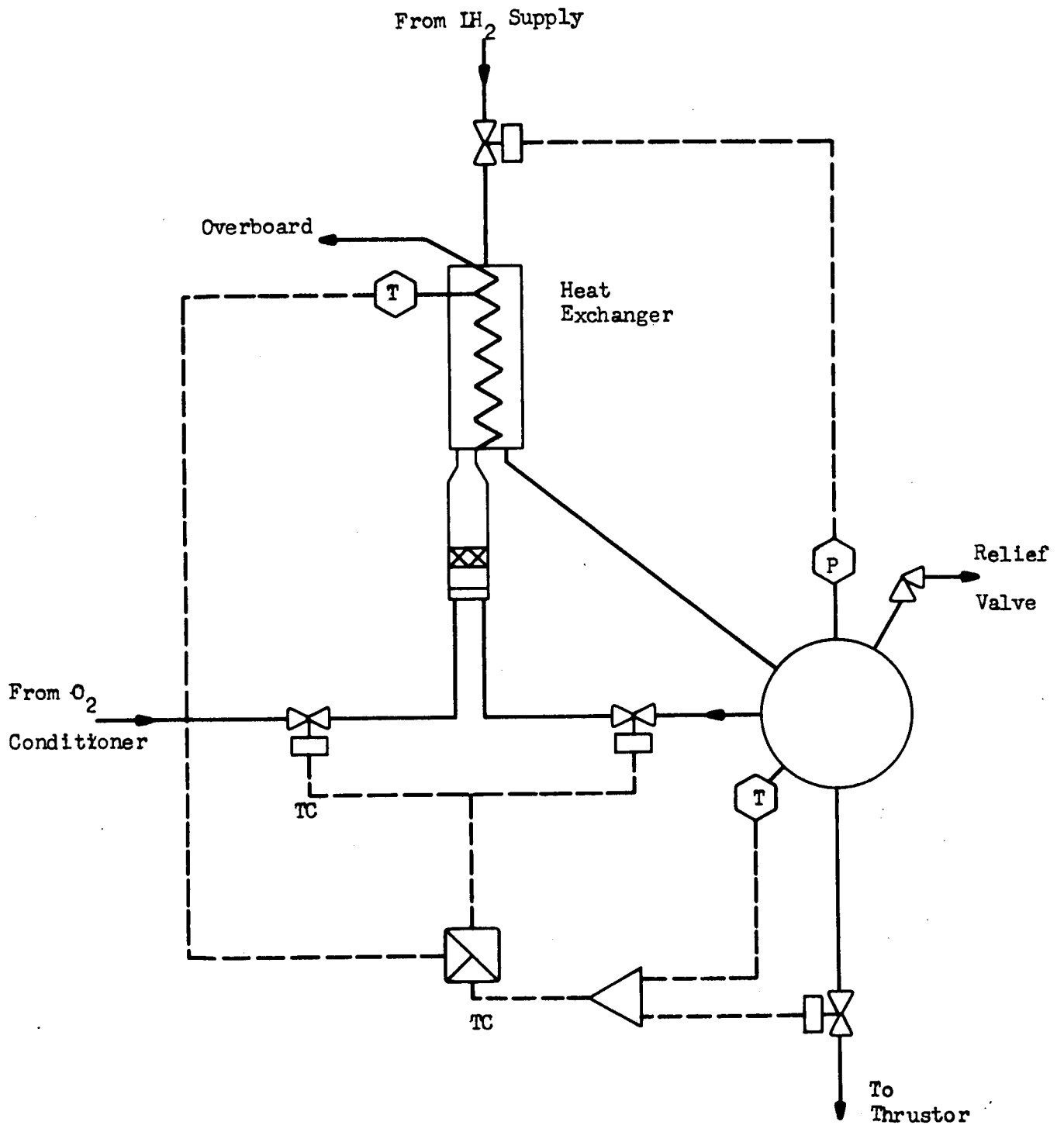Saturated Vapor Inlet and Steady State Thrustor Demand.

Figure 19. Initial Control Scheme for the Heat Exchanger

68

APPENDIX A

CATALYST BED PRESSURE DROP

Initial thrustor computer studies (Fig. 2, Ref. 1) have shown that the catalyst bed pressure drop is a very important engine parameter. This results primarily because of the small pressure head available throughout the system and the need to minimize pressure losses. Thus it was considered desirable to check the approximation by which pressure drop is treated in the thrustor model and to reconsider more theoretical approaches such as the Ergun equation*:

$$\frac{\Delta P \, \rho \, D_p \, g}{L \, Go^2} \frac{\epsilon^3}{1 - \epsilon} = \frac{150 \, (1 - \epsilon)}{\frac{D_p \, Go}{\mu}} + 1.75 \qquad (A-1)$$

where

ϵ = fraction voild volume**

T, MW, and μ = function of the fraction reacted

α (fraction reacted) = A TANH [B (X − C)] + D where A, B, C, D, are selected to approach experimental data

It has unfortunately been found that the pressure drop from the Ergun equation is extremely sensitive to ϵ. However, it has been found that the first term (righthand side, laminar frictional) is 5 to 25 percent of the pressure drop, and if neglected, the equation can be reduced to an orifice type.

---

*R-6342-1, Evaluation and Demonstration of the use of Cryogenic Propellants (O_2-H_2) for Reaction Control Systems, Rocketdyne, a Division of North American Aviation, Inc., Canoga Park, California, 13 October 1965
**A good description of ϵ appears in G. G. Brown and Associates, Unit Operation, John Wiley and Sons, New York, 1950, 215

$$\frac{W}{\epsilon\,A_o} = \sqrt{2g\ \ \rho\ \Delta P\ \frac{D_p}{L}\ \frac{1}{2(1.75)}\ \frac{\epsilon}{1-\epsilon}} \qquad\qquad (A-2)$$

where

$\epsilon\,A_o$ = an effective area

L/D_p = number of orifices

$\dfrac{\epsilon}{1-\epsilon}$ = specific density of orifices.

It was concluded that the technique of treating the catalyst bed as an orifice in the computer model would give reliable results. However, a computer program of the complete Ergun equation has been written using the techniques of Ref. 4 and Ref. 5.

Table A-1 is a summary of calculation using the Ergun equation.

TABLE A-1

SUMMARY OF PRESSURE DROP CALCULATIONS
FROM ERGUN EQUATION
$\epsilon = 0.32$

Condition	Temperature, R	Pressure, psi	Size of Term		$\Delta P/L$
			Laminar	Orifice	psia/in.
Full Flow	200	10	0.0661	1.75	5.32
Full Flow	4050	10	0.676	1.75	124.8
Downstream Infection	2000	10	0.548	1.75	33.9
Downstream Infection	200	10	0.108	1.75	2.81

The parameters from the initial flow test with ambient hydrogen through 1 inch of thrustor bed were measured and hand calculations were made to determine the value of ϵ which gave the measured pressure drop. The resulting value of $\epsilon = 0.45$ was then inserted into the computer program

and the expected pressure drop calculated for the hot test assuming a linear temperature gradient across the first 1/2 inch of catalyst bed, Figure A-1, and A-2.
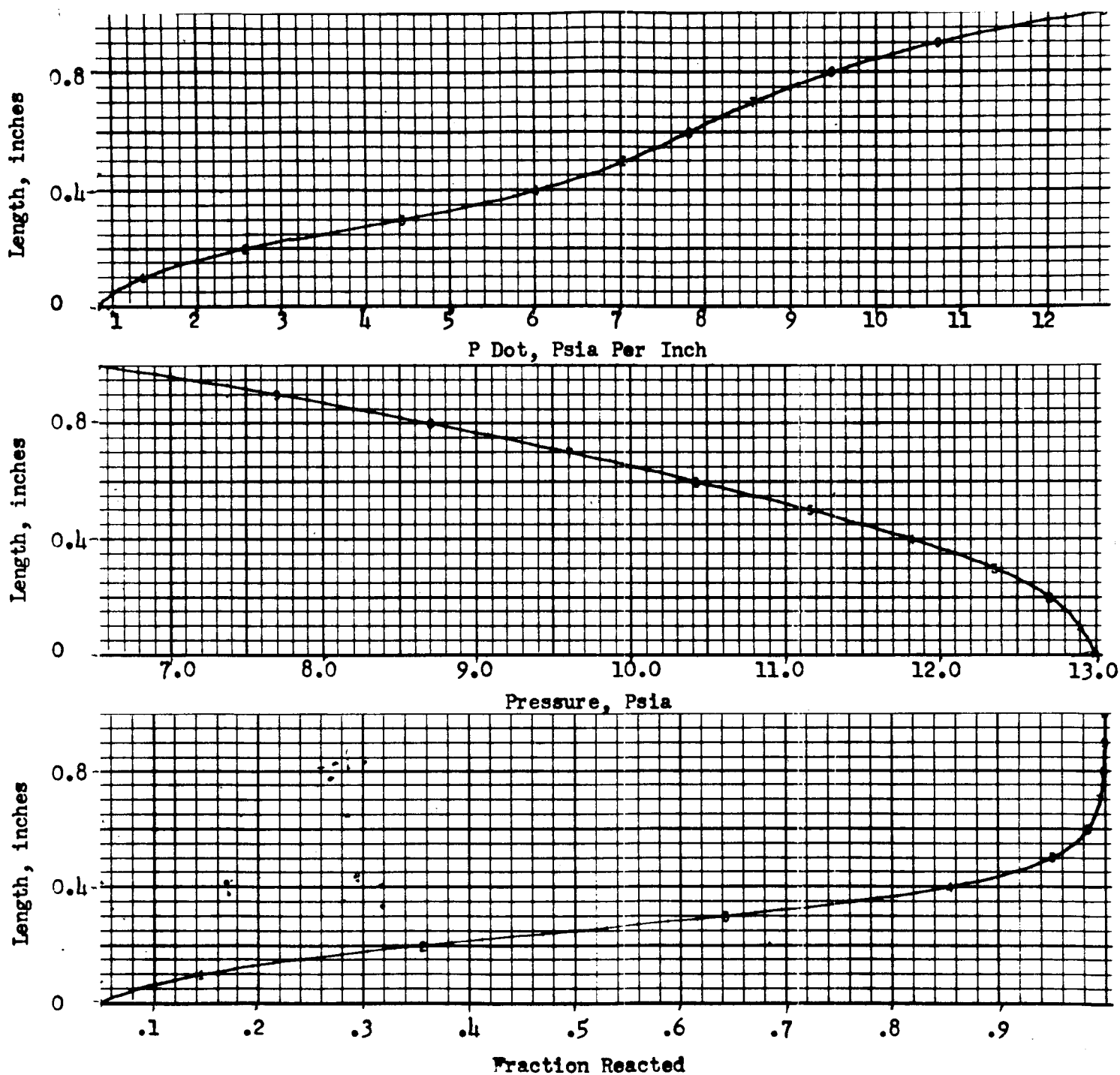
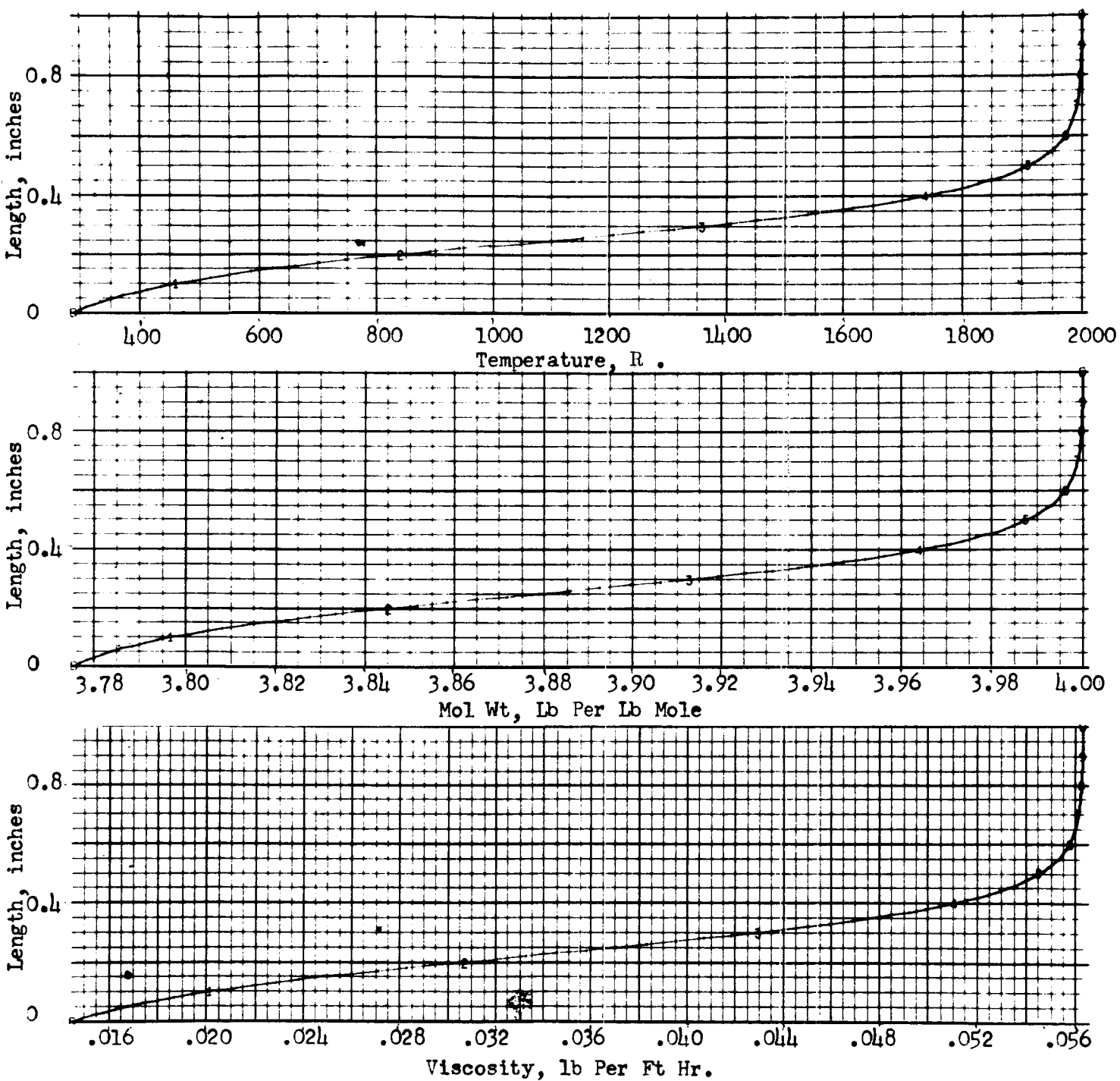Figure A-1. Midas Program Output Describing Pressure Drops From the Ergun Equation

Figure A-2. Midas Program Output Describing Temperature and Viscosity Gradients Using the Ergan Equation

APPENDIX B

FEED PERTURBATION HAND CALCULATIONS

For an oxidizer-rich perturbation of nominal design conditions, the first occurrence is an increase in O_2 flowrate accompanied by a decrease in H_2 flowrate. To a first approximation the flow across the inlet orifices can be assumed sonic, whence the following equation taken from Shapiro* applies:

$$\frac{\dot{w}}{A} = \frac{P_o}{T_o} \sqrt{\frac{kg}{R} \left(\frac{2}{k+1}\right)^{\frac{k+1}{k-1}}} \quad , \quad \frac{P}{P_o} \leq 0.5283 \qquad (B-1)$$

The perturbated flowrate can be calculated from Eq. B-1 by rationing the transient to steady-state flow:

$$\frac{\dot{w}_{O_2}}{\dot{w}_{O_2 \text{ nom}}} = \frac{P_{O_2 \text{ in}}}{P_{O_2 \text{ nom}}} \sqrt{\frac{T_{\text{nom}}}{T_{O_2 \text{ in}}}} \qquad (B-2)$$

$$\frac{\dot{w}_{H_2}}{\dot{w}_{H_2 \text{ nom}}} = \frac{P_{H_2 \text{ in}}}{P_{H_2 \text{ nom}}} \sqrt{\frac{T_{\text{nom}}}{T_{H_2 \text{ in}}}} \qquad (B-3)$$

The new MR is then obtained by dividing Eq. B-2 by Eq. B-3:

$$MR = \frac{P_{O_2 \text{ in}}}{P_{H_2 \text{ in}}} \sqrt{\frac{T_{H_2 \text{ in}}}{T_{O_2 \text{ in}}}} \left(MR_{\text{nom}}\right) \qquad (B-4)$$

New catalyst bed temperatures can then be ready from Fig. 29 of the first quarterly report**. Equation B-4 shows that the change in MR for full flow is greater than for downstream injection.

---

*Shapiro, A.: <u>The Dynamics and Thermodynamics of Compressible Fluid Flow</u>, Vol.1, Ronald Press, New York, 1953.

**R-6342-1, <u>Evaluation and Demonstration of the Use of Cryogenic Propellants for Reaction Control Systems</u>, Rocketdyne, a Division of North American Aviation, Inc., Canoga Park, California, 13 October 1965.

Equation B-2 can be rearranged and solved for the new P_c:

$$P_c = \left(\frac{\dot{w}}{\dot{w}_{nom}}\right)_{throat} \sqrt{\left(\frac{T_c}{T_{nom}}\right)} \, P_{nom} \qquad (B-5)$$

where

$$\left(\frac{\dot{w}}{\dot{w}_{nom}}\right)_{throat} = \frac{\dot{w}_{0_2} + \dot{w}_{H_2}}{0.05} = \frac{(MR + 1)\,\dot{w}_{H_2}}{0.05} \qquad (B-6)$$

Thus it is possible to calculate a new P_c and hence a ΔF. It is interesting to note that ΔF is the same for full flow or downstream injection. The above calculational procedure is illustrated in Table B-1 for the oxidizer-rich case, and the results are summarized in Table B-2 along with other worst-case conditions.

Pressure drop across the valve and the catalyst bed have been ignored in making these calculations. Other assumptions are reversible, adiabatic flow of an ideal gas.

The above procedure has been reworked assuming subsonic flow across the inlet orifices. Shapiro shows, on page 109 of the previously cited treatise, that Eq. B-1 can be rewritten for subsonic flow:

$$\frac{\dot{w}}{A} = \frac{P_o}{\sqrt{T_o}} \left(\frac{P}{P_o}\right)^{1/k} \sqrt{1 - \left(\frac{P}{P_o}\right)^{k-1/k}} \sqrt{\frac{2k}{R\,(k-1)}} \qquad (B-7)$$

where P_o and T_o are propellant inlet conditions and P is the chamber pressure.

The new perturbated H_2 or 0_2 flowrates are given by

$$\frac{\dot{w}_{H_2/0_2}}{\dot{w}_{ss}} = \left(\frac{P_c}{P_{c\ nom}}\right)^{1/k} \left(\frac{P_{in}}{P_{nom}}\right)^{k-1/k} \left(\frac{T_{nom}}{T_{in}}\right) \sqrt{\frac{1-(P_c/P_{in})^{k-1/k}}{\left[1-(P_c/P_{in})\right]^{k-1/k}_{nom}}} \qquad (B-8)$$

EXAMPLE CALCULATION FOR WORST OXIDIZER-RICH CASE

$$\frac{MR}{MR_{ss}} = \frac{P_{0_2}}{P_{H_2}} \sqrt{\frac{T_{H_2}}{T_{0_2}}}_{\text{inlet}} = \frac{17.5}{15.0} \sqrt{\frac{220}{180}} = 1.29$$

$MR_{F.F.} = 2.5 (1.29) = 3.22$, $T_C = 4600$ R (from Fig. 29, page 117, Ref. 4)

MR DSI $= 1.0 (1.29) = 1.29$, $T_C = 2460$ R

$$\frac{\dot{w}_{H_2}}{\dot{w}_{0_{H_2}}} \frac{P_{H_2}}{P_{0_{H_2}}} \sqrt{\frac{T_{0_{H_2}}}{T_{H_2}}} = \frac{15.0}{17.0} \frac{200}{220} = 0.84$$

$$\frac{\dot{w}}{\dot{w}_{ss}}_{\text{throat}} = \frac{(MR + 1)}{0.05} m_{H_2} = \frac{(3.22 + 1)(0.84 \times 0.0143)}{0.05} = 1.014$$

$$P_c = \frac{\dot{w}}{\dot{w}_{ss}} \sqrt{\frac{T_c}{T_{ss}}} P_{ss} = 1.014 \sqrt{\frac{4600}{4050}} (10) = 10.8$$

$$\Delta F = \frac{0.8}{10} \times 100 = 8.0 \text{ percent}$$

TABLE B-2

PERTURBATION CALCULATIONS

P_c Assumed	MR	DSI T_{cat}	T_{cat}	MR	Full Flow T_{cat}	T_{cat}	Throat T_c/T_o	Throat $\dot{w}/\dot{w}_{ss}$	P_c	Thrust, percent
						Upper Oxidizer Rich				
10	1.142	2210	210	2.86	4360	310	1.0387	1.053	10.95	+
									10.81	+8.1
11	1.147	2220	220	2.87	4360	310	1.0387	1.038	10.78	
12	1.16	2260	260	2.90	4370	320	1.0387			
						Worst Oxidizer Rich				
10.0	1.347	2540	540	3.365	4670	620	1.074	1.012	10.89	+8.8
									10.88	
11.0	1.428	2660	660	3.57	4770	720	1.084	1.00	10.88	
12.0	1.488	2760	760	3.72	4850	800	1.094	0.935	10.25	
						Worst Fuel Rich				
10.0	0.744	1560	-440	1.86	3300	-750	0.9028	0.911	8.21	
9.0	0.768	1620	-380	1.92	3370	-680	0.9124	0.909	8.29	+16.4
									8.36	
8.0	0.784	1630	-370	1.96	3420	-630	0.9194	0.915	8.39	
7.0	0.800	1660	-340	1.998	3460	-590	0.9248			
						Upper Fuel Rich				
10.0	0.875	1800	-200	2.19	3710	-340	0.9571	1.018	9.74	-3.4
									9.66	
9.0	0.88	1800	-200	2.20	3710	-340	0.9571	0.996	9.54	
8.0	0.882	1800	-200	2.205	3710	-340	0.9571	0.990	9.46	

This equation is then used to arrive at the perturbated MR:

$$MR = MR_{nom} \left(\frac{P_{O_2}}{P_{H_2}}\right)_{in} \left(\frac{T_{H_2}}{T_{O_2}}\right)_{in} \sqrt{\frac{1-\left(P_c/P_{O_2}\right)_{in}^{k-1/k}}{1-\left(P_c/P_{H_2}\right)_{in}^{k-1/k}}} \qquad (B-9)$$

and the new catalyst bed temperatures.

The calculational procedure is iterative as follows:

1. Assume P_c

2. Calculate MR from Eq. B-9

3. Read new T_{cat} from Fig. 29, page 117, Ref. 9

4. Calculate $\dot{w}_{H_2}/\dot{w}_{ss}$ from Eq. B-8

5. Calculate $\dot{w}/\dot{w}_{nom}$ from Eq. B-6

6. Calculate P_c from Eq. B-5

7. Iterate until P_c assumed = P_c calculated

The calculated results for the four worst-case conditions are presented in Table B-2; compared to the corresponding results from sonic flow, surprisingly small differences are disclosed.

DOCUMENT CONTROL DATA - R&D

(Security classification of title, body of abstract and indexing annotation must be entered when the overall report is classified)

1. ORIGINATING ACTIVITY *(Corporate author)*	2a. REPORT SECURITY CLASSIFICATION
Rocketdyne, a Division of North American Aviation, Inc., 6633 Canoga Avenue, Canoga Park, California	Unclassified
	2b. GROUP

3. REPORT TITLE

Fourth Quarterly Report—Evaluation and Demonstration of the Use of Cryogenic Propellants (O_2-H_2) for Reaction Control Systems

4. DESCRIPTIVE NOTES *(Type of report and inclusive dates)*

Quarterly, 1 April 1966 through 1 July 1966

5. AUTHOR(S) *(Last name, first name, initial)*

N. Weber, F. Hunter, E. Prono, N. Rodewald, G. Haroldsen, A. Liebman, G. Falkenstein

6. REPORT DATE	7a. TOTAL NO. OF PAGES	7b. NO. OF REFS
13 July 1966	78 & xii	12

8a. CONTRACT OR GRANT NO.	9a. ORIGINATOR'S REPORT NUMBER(S)
b. PROJECT NO.	R-6342-4
c.	9b. OTHER REPORT NO(S) *(Any other numbers that may be assigned this report)*
d.	

10. AVAILABILITY/LIMITATION NOTICES

11. SUPPLEMENTARY NOTES	12. SPONSORING MILITARY ACTIVITY
	NASA Lewis Research Center Cleveland, Ohio

13. ABSTRACT

A 16-month applied research program is being conducted with the overall objectives of evaluating and demonstrating the feasibility of a cryogenic reaction control system (RCS) and exploring possible problem areas of such a system. The RCS is divided into two subsystems. One subsystem is to condition the propellants to a given thermodynamic state regardless of the inlet state; the other subsystem consists of the thrustors. The program consists of six integrated tasks (an initial concept design-analytical effort; a design, fabrication, and test plan formulation effort; and an experimental-analytical effort for each subsystem) as follows: I. Thrustor Analysis and Conceptual Design, II. Conditioner Analysis and Conceptual Design, III. Thrust Design and Fabrication, IV. Conditioner Design and Fabrication, V. Thrust Evaluation Tests, VI. Conditioner Evaluation Tests. The first two tasks have been completed, and the requisite concept review and approvals have been obtained from the NASA technical monitor.

DD FORM 1 JAN 64 **1473**

| 14. | LINK A | | LINK B | | LINK C | |
KEY WORDS	ROLE	WT	ROLE	WT	ROLE	WT
Catalytic Ignition						
Cryogenic Attitude Control Systems						
Catalytic Thrustor Design						
Los Pressure						

INSTRUCTIONS

1. **ORIGINATING ACTIVITY:** Enter the name and address of the contractor, subcontractor, grantee, Department of Defense activity or other organization *(corporate author)* issuing the report.

2a. **REPORT SECURITY CLASSIFICATION:** Enter the overall security classification of the report. Indicate whether "Restricted Data" is included. Marking is to be in accordance with appropriate security regulations.

2b. **GROUP:** Automatic downgrading is specified in DoD Directive 5200.10 and Armed Forces Industrial Manual. Enter the group number. Also, when applicable, show that optional markings have been used for Group 3 and Group 4 as authorized.

3. **REPORT TITLE:** Enter the complete report title in all capital letters. Titles in all cases should be unclassified. If a meaningful title cannot be selected without classification, show title classification in all capitals in parenthesis immediately following the title.

4. **DESCRIPTIVE NOTES:** If appropriate, enter the type of report, e.g., interim, progress, summary, annual, or final. Give the inclusive dates when a specific reporting period is covered.

5. **AUTHOR(S):** Enter the name(s) of author(s) as shown on or in the report. Enter last name, first name, middle initial. If military, show rank and branch of service. The name of the principal author is an absolute minimum requirement.

6. **REPORT DATE:** Enter the date of the report as day, month, year; or month, year. If more than one date appears on the report, use date of publication.

7a. **TOTAL NUMBER OF PAGES:** The total page count should follow normal pagination procedures, i.e., enter the number of pages containing information.

7b. **NUMBER OF REFERENCES:** Enter the total number of references cited in the report.

8a. **CONTRACT OR GRANT NUMBER:** If appropriate, enter the applicable number of the contract or grant under which the report was written.

8b, 8c, & 8d. **PROJECT NUMBER:** Enter the appropriate military department identification, such as project number, subproject number, system numbers, task number, etc.

9a. **ORIGINATOR'S REPORT NUMBER(S):** Enter the official report number by which the document will be identified and controlled by the originating activity. This number must be unique to this report.

9b. **OTHER REPORT NUMBER(S):** If the report has been assigned any other report numbers *(either by the originator or by the sponsor)*, also enter this number(s).

10. **AVAILABILITY/LIMITATION NOTICES:** Enter any limitations on further dissemination of the report, other than those imposed by security classification, using standard statements such as:

(1) "Qualified requesters may obtain copies of this report from DDC."

(2) "Foreign announcement and dissemination of this report by DDC is not authorized."

(3) "U. S. Government agencies may obtain copies of this report directly from DDC. Other qualified DDC users shall request through

_____ ."

(4) "U. S. military agencies may obtain copies of this report directly from DDC. Other qualified users shall request through

_____ ."

(5) "All distribution of this report is controlled. Qualified DDC users shall request through

_____ ."

If the report has been furnished to the Office of Technical Services, Department of Commerce, for sale to the public, indicate this fact and enter the price, if known.

11. **SUPPLEMENTARY NOTES:** Use for additional explanatory notes.

12. **SPONSORING MILITARY ACTIVITY:** Enter the name of the departmental project office or laboratory sponsoring *(paying for)* the research and development. Include address.

13. **ABSTRACT:** Enter an abstract giving a brief and factual summary of the document indicative of the report, even though it may also appear elsewhere in the body of the technical report. If additional space is required, a continuation sheet shall be attached.

It is highly desirable that the abstract of classified reports be unclassified. Each paragraph of the abstract shall end with an indication of the military security classification of the information in the paragraph, represented as *(TS), (S), (C),* or *(U).*

There is no limitation on the length of the abstract. However, the suggested length is from 150 to 225 words.

14. **KEY WORDS:** Key words are technically meaningful terms or short phrases that characterize a report and may be used as index entries for cataloging the report. Key words must be selected so that no security classification is required. Identifiers, such as equipment model designation, trade name, military project code name, geographic location, may be used as key words but will be followed by an indication of technical context. The assignment of links, rules, and weights is optional.